

Manuscript Number:

Title: Sequence stratigraphy after the demise of a high-relief carbonate platform (Carnian of the Dolomites): sea-level and climate disentangled

Article Type: Research Paper

Keywords: Sequence stratigraphy; carbonate platform demise; climate change; Dolomites; Triassic.

Corresponding Author: Mr. Giovanni Gattolin,

Corresponding Author's Institution: University of Padova

First Author: Giovanni Gattolin

Order of Authors: Giovanni Gattolin; Nereo Preto, Ph.D.; Anna Breda, Ph.D.; Marco Franceschi, Ph.D.; Matteo Isotton; Piero Gianolla, Ph.D.

Abstract: In this contribution sedimentary facies analysis and geological 3D modeling are applied to constrain the sequence stratigraphy of a complex stratigraphic interval in the Late Triassic of the Dolomites and allow to highlight the interaction of sea level and climate changes. This multidisciplinary approach was key to disentangle the timing of climatic change vs. sea level fluctuation and their effects on a shallow water carbonate depositional system. The "Carnian Pluvial Event", a global episode of climate change worldwide documented at low latitudes, involved increased rainfall and possibly global warming. This climatic event, predates a drop of sea-level and caused the demise of microbial-dominated high-relief carbonate platforms that dominated the Dolomites region and was followed by a period characterized by the coexistence of small microbial carbonate mounds and loose arenaceous carbonates. A subsequent sea level fall brought to the definitive disappearance of microbialites and shallow water carbonates switched to ramps dominated by loose carbonate sediment. The climate-induced crisis of Early Carnian shallow water carbonate systems of the Dolomites generated a geological surface similar to a drowning unconformity, although no transgression occurred. The sudden infilling of basins at the end of the Early Carnian was the result of the climatic-induced switch from high-relief carbonate systems characterized by steep slopes to a gently inclined ramp, rather than by the continuous progradation of a high-relief microbial platform. Results show that the evolution of carbonate systems of the Dolomites at the end of the Early Carnian cannot be interpreted in the light of sea level changes only, pointing out that ecological changes can induce significant modifications in depositional geometries. This case study may serve as a conceptual model for the sedimentary evolution of carbonate systems subject to ecological crisis that do not evolve in platform drowning because of a lack of accommodation.

Suggested Reviewers: Andr  Strasser Ph.D.
Prof. Em., Dept. of Geosciences, Universit  de Fribourg
andreas.strasser@unifr.ch
Broad experience on sequence stratigraphy applied to carbonate systems

Jeroen Kenter Ph.D.
Statoil ASA
kenter.jeroen@gmail.com

Expert of carbonate systems, already worked on sequences similar to those described in this paper

Sven Egenhoff Ph.D.

Prof., Dept. of Geosciences, Colorado State University

Sven.Egenhoff@colostate.edu

Expert of carbonate systems, published several papers on high-relief carbonate platforms of the Triassic of the Dolomites

Daniel J Lehrmann Ph.D.

Prof., Dept. of Geosciences, Trinity University

dlehrmann@trinity.edu

Broad experience on carbonate realms, worked on Triassic carbonate platforms of China.

Padova, February 24th, 2014

Prof. David J. Bottjer
Palaeogeography, Palaeoclimatology, Palaeoecology
Editor

I submit for your kind attention the manuscript entitled “Sequence stratigraphy after the demise of a high-relief carbonate platform (Carnian of the Dolomites): sea-level and climate disentangled”, with the hope that it can be published in Palaeogeography, Palaeoclimatology, Palaeoecology.

I believe that this contribution is of interest for the broad community of earth scientists, as it brings new data useful to constrain the sequence stratigraphy of a complex stratigraphic interval in the Late Triassic of the Dolomites allowing to further detail the effects of the interaction of sea level and climate changes on carbonate platform systems.

The study has been carried out coupling facies analysis and 3D geological modeling techniques. This multidisciplinary approach was key to disentangle the timing and interaction of climatic change vs. sea level fluctuation.

The evolution of the sedimentary system described in this paper can be summarized as follows: A worldwide documented Late Triassic climatic event increased rainfall and possibly led to global warming triggering the demise of the microbial-dominated high-relief carbonate platforms of the Dolomites. After this event, a period of coexistence of small microbial carbonate mounds and loose arenaceous carbonates is documented. A subsequent sea level fall brought to the complete disappearance of microbialites and shallow water carbonates switched to ramps dominated by associations typical of a cool-water factory mixed with siliciclastic sediment.

The climate-induced crisis of microbial-dominated high-relief carbonate platforms generated a geological surface similar to a drowning unconformity, although no transgression was involved. This observation highlights a known caveat of the sequence stratigraphy of carbonates: ecological changes determine significant changes in depositional geometries, and so the evolution of carbonate systems cannot be interpreted or predicted on the basis of the observations of sea level change only. This case study may serve as conceptual model for the interpretation of the evolution of carbonate system in times of ecological crisis.

Sincerely,

Giovanni Gattolin
(on behalf of all authors)

Facies analysis and geological 3D modeling applied to constrain sequence stratigraphy

A multidisciplinary approach to disentangle climatic vs. sea level change effects

The switch from microbial to cool-water factory results triggered by climate change

A carbonate system subject to ecological crisis that does not evolve in a drowning

Generation of a surface similar to a drowning unconformity without a transgression

1 **Sequence stratigraphy after the demise of a high-relief carbonate platform**
2 **(Carnian of the Dolomites): sea-level and climate disentangled.**

3

4 Gattolin G.*¹, Preto N.¹, Breda A.¹, Franceschi M.², Isotton M.¹ and Gianolla P.³

5

6 1 - Department of Geosciences, University of Padova, Italy

7

2 - Museo delle Scienze, Trento, Italy

8

3 - Department of Physics and Earth Sciences, University of Ferrara, Italy

9

* - Corresponding author. Mail: gio.gattolin@gmail.com

10

11 **Abstract**

12

13 In this contribution sedimentary facies analysis and geological 3D modeling are applied to constrain
14 the sequence stratigraphy of a complex stratigraphic interval in the Late Triassic of the Dolomites
15 and allow to highlight the interaction of sea level and climate changes. This multidisciplinary
16 approach was key to disentangle the timing of climatic change vs. sea level fluctuation and their
17 effects on a shallow water carbonate depositional system. The “Carnian Pluvial Event”, a global
18 episode of climate change worldwide documented at low latitudes, involved increased rainfall and
19 possibly global warming. This climatic event, predates a drop of sea-level and caused the demise of
20 microbial-dominated high-relief carbonate platforms that dominated the Dolomites region and was
21 followed by a period characterized by the coexistence of small microbial carbonate mounds and
22 loose arenaceous carbonates. A subsequent sea level fall brought to the definitive disappearance of
23 microbialites and shallow water carbonates switched to ramps dominated by loose carbonate
24 sediment. The climate-induced crisis of Early Carnian shallow water carbonate systems of the
25 Dolomites generated a geological surface similar to a drowning unconformity, although no

26 transgression occurred. The sudden infilling of basins at the end of the Early Carnian was the result
27 of the climatic-induced switch from high-relief carbonate systems characterized by steep slopes to a
28 gently inclined ramp, rather than by the continuous progradation of a high-relief microbial platform.
29 Results show that the evolution of carbonate systems of the Dolomites at the end of the Early
30 Carnian cannot be interpreted in the light of sea level changes only, pointing out that ecological
31 changes can induce significant modifications in depositional geometries. This case study may serve
32 as a conceptual model for the sedimentary evolution of carbonate systems subject to ecological
33 crisis that do not evolve in platform drowning because of a lack of accommodation.

34

35 **Key Words**

36

37 Sequence stratigraphy, carbonate platform demise, climate change, Dolomites, Triassic.

38

39 **1. Introduction**

40 Sequence stratigraphy is a powerful tool to understand the history and the evolution of depositional
41 systems and sedimentary basins (e.g., Vail et al., 1991; Catuneanu, 2006; Catuneanu et al., 2011). It
42 has been successfully applied in a variety of geodynamic settings to both siliciclastic (Galloway and
43 Williams 1991; Helland-Hansen 1992; Mellere and Steel 1995; Miall and Arush 2001; Catuneanu et
44 al., 2002; Cantalamessa et al., 2005; Breda et al., 2009a; Galloway 2008; Miall et al., 2008; among
45 others) and carbonate systems (De Zanche et al. 1993; Pasquier and Strasser 1997; Gianolla et al.
46 1998; Gianolla and Jacquin 1998; Pomar and Tropeano 2001; Mateu-Vicens et al., 2008; among
47 others). However, the sequence stratigraphic interpretation of carbonate systems still has significant
48 limitations, related to the capability of some carbonate platforms to produce sediment in situ, at a
49 rate that is influenced by oceanographic and climatic parameters more than by sea level change
50 (Schlager, 1991; 1993; Schlager et al., 1994; Pomar, 2001). One singularity of carbonate platforms
51 is that they can drown, that is, the platform top can be submerged below the photic zone; in that

52 case, the platform cannot catch up to sea level and the carbonate production is irreversibly shut
53 down (Schlager 1981; 1999a, b; Hallock and Schlager 1986). The geometry and facies of drowned
54 carbonate platforms mime a rise of the sea level even during periods of sea level stability. In the
55 specific case of carbonate platforms drowning, the special behavior of carbonate systems has been
56 often related to a change in the ecology or biology of carbonate producers, in turn commonly linked
57 to climate and/or environmental changes (Schlager 1981; Hallock and Schlager 1986; Jenkyns
58 1991; Mutti et al. 1997, 2005; Weissert et al. 1998; Wilson et al. 1998; Mutti and Hallock 2003;
59 Schlager 2003; Pomar et al., 2004; Föllmi and Godet 2013; Godet et al. 2013; among others). In the
60 Triassic of the Dolomites (North-eastern Italy, Fig. 1a), sedimentary sequences are dominated by
61 carbonates. During the last decades, several sequence stratigraphic interpretations of these
62 successions were proposed (Brandner, 1984; De Zanche et al., 1992; De Zanche et al., 1993;
63 Ruffner and Zühlke, 1995; Neri and Stefani, 1998; Gianolla et al. 1998; Neri et al., 2007) that had
64 to face the paradox of drowning platforms, at times of prolonged and intense subsidence as the
65 Middle Triassic (De Zanche et al., 1995; Blendinger et al., 2004; Preto et al., 2005; Brack et al.,
66 2007).

67

68 At the end of the early Carnian, a major event of carbonate platform demise is recorded in the
69 Dolomites: carbonate production in high-relief platforms suddenly shuts off and is replaced by the
70 deposition of mixed carbonate-siliciclastic sediments deposited on a low-relief ramp depositional
71 profile (Heiligkreuz Formation in Neri et al 2007, ex Dürrenstein Formation of De Zanche et al.,
72 1993; Preto and Hinnov, 2003; Bosellini et al., 2003; Stefani et al., 2010; Fig. 2). This crisis of
73 high-relief carbonate platforms is not confined to the Dolomites. In fact, it was initially identified in
74 the Northern Calcareous Alps of Austria (Schlager and Schöllenderger, 1974) and then recognized
75 at the scale of the Tethys ocean (e.g., Simms et al., 1995; Hornung et al., 2007a; Preto et al., 2010).
76 This crisis is now considered as one of the many effects of a global episode of climate change, the
77 "Carnian Pluvial Event" (CPE) of Simms and Ruffell (1989). The CPE corresponds to an increase

78 in rainfall and runoff at low latitudes, reflected in sedimentological, geochemical and palynological
79 proxies (e.g., Simms and Ruffel, 1989, 1990; Simms et al., 1995; Roghi, 2004; Prochnow et al.,
80 2006; Preto et al., 2010; Nakada et al., 2014), triggered by a major perturbation of the global carbon
81 cycle (Dal Corso et al., 2012). Oxygen isotopes of conodont apatite also suggest that the CPE
82 corresponds to an episode of global warming (Hornung et al., 2007b; Rigo and Joachinski, 2010).
83 The onset of the CPE is tightly constrained in the area of Rifugio Dibona (Dal Corso et al., 2012),
84 where the outcrops considered in this study are located.

85

86 In the Dolomites, the interpretation of the stratigraphic interval around the CPE, in terms of
87 sequence stratigraphy, is challenging. In literature the ramp deposits formed after the demise of
88 high-relief early Carnian platforms are interpreted as a complete 3rd order depositional sequence.
89 The sea level fall at the base of this interval is considered the cause of the demise of these carbonate
90 platforms (De Zanche et al. 1993; Gianolla et al. 1998; Bosellini et al., 2003). However, this
91 interpretation does not explain the change in the type of carbonate sediments and is incongruous
92 with most episodes of carbonate platform drowning of the Mesozoic (Schlager, 1981; 1999a, b;
93 2005; Weissert et al., 1998). The suite of climatic and geochemical changes recorded at the CPE,
94 and its global rather than regional distribution, are in fact remarkably similar to those of major
95 Mesozoic Oceanic Anoxic Events (Preto et al., 2010). These events are associated to ecological
96 crises of carbonate platforms, including commonly their drowning (e.g, Jenkyns, 1985; 1991;
97 Weissert et al., 1998; Léonide et al., 2012).

98 In this work, a reappraisal of the sequence stratigraphy of the Heiligkreuz Formation (youngest
99 early Carnian) is endeavored in the light of the analogy between the CPE and other Mesozoic
100 perturbations of the carbon cycle, and their effects on carbonate platforms. The focus is put on the
101 sequence boundary at the base of the Heiligkreuz Formation, with the aim of disentangling the roles
102 of sea level change and environmental factors on the demise of the underlying high-relief carbonate
103 platforms. To this end we applied 3D modeling techniques coupled with facies analysis to assess the

104 relative timing of the platform demise with respect to the sedimentary record of sea level fall and
105 subaerial exposure. Our data suggest that the demise of high-relief carbonate platforms occurred
106 before sea level fall and the consequent subaerial exposure; depositional geometries mimicking a
107 sequence boundary were thus generated and are unrelated to an actual decrease in accommodation,
108 in analogy to typical drowning unconformities (type 3 SB of Schlager, 1999b). Differently from
109 episodes of drowning of the Middle Triassic, however, the CPE and the related demise of high-
110 relief carbonate platforms occurred at a time of tectonic quiescence, at the end of a long-term
111 depositional cycle (Gianolla and Jacquin, 1998), when accommodation in the area was created at a
112 slow rate. The case study of the Carnian of the Dolomites thus shows that climate-induced crises of
113 carbonate systems can generate surfaces similar to drowning unconformities not related to times of
114 prolonged transgression.

115

116 **2. Geological setting**

117 During the Middle-Late Triassic, the Dolomites (North-eastern Italy, Fig. 1a) were located in the
118 western portion of the Tethys Ocean (Ziegler, 1988; Dercourt et al., 1993) at northern tropical
119 latitudes (Fig. 1b; Muttoni et al., 1996; Broglio Loriga et al., 1999; Flügel, 2002). The area was
120 characterized by a “chess-board-like” paleotopography featuring domains with different subsidence
121 rates (horsts and grabens) and bounded by roughly North-South and East-West faults (Masetti and
122 Neri, 1980; Blendinger, 1986; De Zanche 1993; Gianolla et al., 1998; Preto et al., 2011). Often,
123 horsts hosted the onset of isolated high-relief carbonate platforms dominated by Microbial to
124 Tropical carbonate factories (*sensu* Schlager 2003), while in grabens a carbonate to siliciclastic
125 basinal sedimentation took place (Masetti e Neri 1980; Gaetani et al., 1981; Bosellini 1984;
126 Bosellini et al. 2003; Neri et al. 2007; Preto et al. 2011; among others). Toward the end of the early
127 Carnian, a progressive slowdown of the high subsidence rates along with a strong siliciclastic input
128 to marginal basins resulted in the flattening of this complex paleotopography. Contemporaneously,
129 an important turnover in carbonate factories and carbonate platform geometries occurred and

130 Microbial to Tropical factories were replaced by Cool-water to Tropical factories (*sensu* Schlager,
131 2003) which originated ramp geometries (Bosellini et al., 2003; Preto and Hinnov, 2003; Stefani et
132 al., 2010). The demise of the last generation of high-relief Carnian carbonate platforms (Fig. 2;
133 Cassian 2 platforms in De Zanche et al. 1993) is attributed to two main factors: (1) the subaerial
134 exposure they suffered following an important sea level drop and (2) the considerable siliciclastic
135 input (in turn triggered by the sea level drop) which can be detrimental to the carbonate production
136 (Russo et al., 1991; Keim et al., 2001; Bosellini et al., 2003). This sea level drop constitutes the
137 lower sequence boundary of a third order depositional sequence (Fig. 2; Car 3 in De Zanche et al.
138 1993; Gianolla et al., 1998), object of this study.

139

140 **3. Methods**

141 A three-dimensional model of the southern walls of Tofana di Rozes (see Fig. 1a for location; Fig
142 3a) was created with the photogrammetric software Agisoft™ Photoscan. Forty-six highly
143 overlapping photographs were taken from a working distance of ~ 4 km using a Sony α 200 DSLR
144 camera (resolution = 10.2 megapixel) coupled with a Minolta AF 100-200 f4.5 zoom lens (selected
145 focal length = 100mm, $f = 9$). To scale and georeference the model 20 GPS points, well
146 recognizable both on the field and on the photographs, were taken with the aid of a Royaltek RBT-
147 2200 bluetooth GPS (average uncertainty in the specific conditions ~ 1 – 5 m) coupled with a HP
148 iPAQ 214 handheld pc running Esri® ArcPAD™ 7.0. A three-dimensional model of the Dibona
149 Hut outcrop (Fig. 1a for location; Fig. 4a) was acquired through an Optech Ilris 3D terrestrial laser
150 scanner (wavelength 1500 nm, acquisition speed 2500 points per second). The working distance
151 was ~ 60 m and the resolution of the point clouds is ~ 1 point every 4 cm. To georeference the
152 model, the GPS position of 6 targets was taken using a high precision Base-Rover Topcon HiPer®
153 Pro system (uncertainty ~ 3 cm).

154 Sedimentary facies were defined in the field and through petrographic analysis, using standard
155 sedimentology methods (e.g., Tucker and Wright, 1990; Flügel, 2004).

156

157 **4. Lithozones**

158

159 The sedimentary succession was divided into six lithozones. Each of these lithozones is
160 characterized by a different facies association, stratal patterns and depositional geometries. A brief
161 description of lithozones is provided below; for a more detailed description the reader is referred to
162 Preto and Hinnov (2003) and Gattolin et al. (2013).

163

164 Lithozone 1 (L-1)

165

166 This lithozone was observed only at Tofana di Rozes, where it constitutes a wedge pinching out
167 toward the East. Its maximum thickness is ~ 200 m on the western side of the outcrop (Figs. 3b, c).
168 It is mainly constituted by m thick clinofolds of pervasively dolomitized limestone. Locally
169 megabreccias, with m to tens of m large boulders, were identified. Dolomitization hampers the
170 observation of original facies. L-1 pertains to the platform slope of one of the Carnian high-relief
171 carbonate platforms (Cassian 2 of De Zanche et al. 1993; Gianolla et al 1998). The correspondent
172 margin and platform top facies are not observable in the Dibona and Tofane area, but have been
173 described in neighboring outcrops at Falzarego Pass (Fig. 1a; Breda et al., 2009b). The microbial
174 character of these platforms is known, however, from allochthonous boulders and carbonate grains in
175 the adjacent basins (Russo et al., 1997; Keim and Schlager, 1999; 2001; Preto, 2012). Except for the
176 toe of slope portion, which is often characterized by megabreccias, they are dominated by microbial
177 boundstones.

178

179 Lithozone 2 (L-2)

180

181 The boundary between the first and the second lithozone was observed at Tofana di Rozes. It is
182 constituted by a sharp, ~ E dipping by-pass surface on top of the last slope clinoform of L-1. L-2 is
183 constituted by lenticular-shaped carbonate bodies (mounds) mainly made up of microbial
184 boundstone (Figs. 3b, c; 5), interlayered and laterally onlapped by dm thick beds of arenaceous
185 grainstones with bivalves, gastropods, peloids, plant remains (Fig. 6). Mounds are the dominant
186 facies at Tofana di Rozes, where they present maximum size (10-100 m), while arenaceous
187 grainstones prevail at Dibona Hut (Fig. 5; 6). Cm- dm thick beds of calcsiltite and shale are rare at
188 both localities (Fig. 7).

189 At Dibona Hut, the last part of this lithozone is constituted by a ~ 3 m thick sequence of m-scale
190 beds with a highly erosive base, made up of arenaceous-conglomeratic grainstones (main
191 components are volcanic rock fragments, quartz, molluscs, echinoderms, plant debris and rare
192 amber droplets; Breda et al., 2009b) which testifies the onset of mass flows. These coarse grained
193 beds are overlaid by a 30 m thick clinostratified body (L-2-CLINO in Fig. 4c) which dm-scale beds
194 are essentially made up of arenaceous grainstone (main components are bivalves, gastropods,
195 peloids, plant remains and echinoderms), with plane parallel bed joints. Beds are grouped in bedsets
196 which present foresets dipping ~ 25° toward the E (after correction of tectonic tilt) and topsets
197 progressively lowered toward the E (Fig. 4c). These clinostratified bedsets represent the two-
198 dimensional along-dip cut of a sedimentary body which along-strike geometry is not visible due to
199 exposure bias. As the three dimensional geometry of clinoforms is not observable, it is not possible
200 to actually interpret the sedimentary body. The high dip-angle of the beds and the amplitude of the
201 bedsets constrain the shortlist to two possibilities: a delta (implying an along-strike lobate shape of
202 clinoforms) or a coastal prograding wedge (implying an along-strike rectilinear shape of
203 clinoforms), but a further distinction between them is not possible. The clinostratified body is
204 onlapped by tabular dm to m beds of often dolomitized arenaceous grainstone (L-2-ONLAP in Fig.
205 4c).

206

207 Lithozone 3 (L-3)

208

209 This lithozone consists of an alternation of dm to m thick dolostone beds, with peloids, often
210 capped by stromatolitic lamination, sheet cracks and planar fenestrae, and dm-scale calcarenite
211 beds. Both facies are characterized by burrows and by a rooted or karstic horizon at the top of the
212 beds. Over the karstified top of some beds, thin layers of dark clays and shales are present and
213 display roots, plant fragments, amber, pyrite and coal. Rare dm beds of massive arenites were
214 observed and among them the most evident are located in the lower portion of this lithozone. This
215 stacking of facies suggests a peritidal/paralic environment (see interval D of Preto et al. 2003 and
216 interval 1 of Gattolin et al. 2013). Dolostones and grainstones represent the normal peritidal cycles,
217 clays and shales the development of littoral swamps (paralic). Massive arenites are rare episodes of
218 high continental sediment discharge into the basin while some of them represent lags. At Tofana di
219 Rozes, the boundary between L-2 and L-3 is marked by a well developed karstic surface that toward
220 the West interests also L-1 (Fig. 8). At Dibona Hut, L-3 directly overlies L-2-ONLAP and no
221 evidences of karstification have been observed between them.

222

223 Lithozone 4 (L-4)

224

225 The limit between the third and the fourth lithozone is gradational. Due to the absence of a sharp
226 boundary between them it has been arbitrary placed at the first occurrence of well developed planar
227 cross stratification within the succession. Those sedimentary structures are common in L-4 and
228 were observed in dm thick beds, mainly made up of oolitic-bioclastic calcarenites. Sets of laminae
229 alternately migrating in two opposing directions can be found. Dm-scale beds of fine to medium
230 grained arenite, mainly made up of quartz, chert, feldspar and lithic grains are also observed, with
231 local presence of cm to dm-scale cross stratification, at times migrating in two opposing directions.

232 Levels of imbricated bivalve shells (Coquina) can be found at the base of calcarenites and arenites.
233 Dm thick beds of calcsiltites to calcarenites with mud interbeds, characterized by the presence of
234 ripples, are common. The most represented grains in this facies are peloids. The general structure of
235 this facies is flaser-bedding to wavy-bedding as a function of variable mud content. Cm- dm thick
236 beds of dark shales and siltites rich in plant remains are locally characterized by the presence of
237 isolated ripples made up of calcarenites, producing lenticular bedding. White wackestone to grey
238 marly wackestone, not showing sedimentary structures, and massive dm beds of mixed carbonate-
239 siliciclastic to pure siliciclastic arenites, were rarely observed. The whole L-4 is often interested by
240 burrows. The facies stacking pattern suggests that L-4 deposited in a subtidal environment.
241 Calcarenites and arenites with planar cross bedding and foresets alternatively migrating in opposing
242 directions, as well as flaser to wavy to lenticular bedding, indicate that the dominant mechanism of
243 sediment transport was reversing tidal currents. Episodes of subaerial exposure are almost absent
244 (see interval 2 of Gattolin et al., 2013 for details).

245

246 Lithozone 5 (L-5)

247

248 The boundary between L-4 and L-5 is gradational, it has been placed at the complete disappearance
249 of tractional sedimentary structures. L-5 consists of dm to m thick nodular beds of often
250 dolomitized limestones and marly limestones. Ammonoids and conodonts were found at Dibona.
251 Some ammonoids were collected also in the Col dei Bos area, ~ 500 m West of Tofana di Rozes
252 (Preto and Hinnov, 2003; Breda et al., 2009b). Cm to dm beds of gray marls with *Chondrites* and
253 locally with pyrite nodules were locally observed. The absence of tractional sedimentary structures
254 and of evidences of subaerial exposure, together with the nodular bed joints and the fossils content
255 (ammonoids), suggest a completely subtidal origin for this lithozone, deeper than L-4, and a
256 temporary partial starvation of the system (see interval 3 of Gattolin et al., 2013 for details).

257

258 Lithozone 6 (L-6)

259

260 The sixth lithozone (L-6, Figs. 3c and 4c) consists of ~ 30 m of massive dolostone. Sedimentary
261 structures are obliterated by dolomitization, only ooids are locally recognizable. Observations on
262 the same interval carried out by Gattolin et al. (2013, see their interval 4) on outcrops neighboring
263 the Dibona and Tofane area, reveal the presence of dm to m thick beds of dolostones (Lastoni di
264 Formin; Fig. 1a) and mixed oolitic-siliciclastic arenites (Falzarego Pass, Valparola Pass, Lastoni di
265 Formin; Fig. 1a) with planar cross bedding and herringbone cross bedding. The absence of subaerial
266 exposure surfaces and the presence of planar and herringbone cross bedding suggest that L-6
267 deposited in a subtidal environment, dominated by tidal currents. The top of L-6 is marked in the
268 whole area by a well developed karstic surface (Fig. 9).

269

270 Lithozone 7 (L-7)

271

272 This lithozone (L-7; Figs. 3c and 4c) consists of dm thick beds of aphanitic, mottled dolostones
273 alternated to dark clays and represents a marginal marine/paralic environment. L-7 constitutes the
274 basal part of the Travenanzes Formation, a mixed siliciclastic/carbonate succession of alluvial plain
275 to floodbasin to tidal flat environments that deposited during Upper Carnian on a wide, low-relief
276 coastal area (Breda and Preto, 2011).

277

278 **5. Sequence stratigraphy**

279

280 The described succession, together with observations made on stratal patterns, depositional
281 geometries and erosional surfaces led to disentangle the sequence stratigraphy of the studied
282 interval. The sequence stratigraphic interpretation of the succession is provided below using the
283 standard terminology of Catuneanu et al. (2009; 2011). As in the previous sequence stratigraphic

284 interpretations of this interval (De Zanche et al., 1993; Gianolla et al., 1998) and according to Vail
285 et al. (1991), the sequence boundary is placed at the base of the falling stage systems tract .

286

287 **5.1 1st depositional sequence**

288

289 Highstand systems tract

290

291 The pervasively dolomitized clinostratified sedimentary body outcropping at the base of the Tofana
292 di Rozes (L-1; Fig. 3) represents the slope of the last Carnian high-relief carbonate platforms in the
293 Dolomites area (Cassian 2 of De Zanche et al. 1993; Gianolla et al. 1998). In terms of geometry, the
294 toe of slope rapidly advances basinward. The shoreline trajectory, which is marked by the trajectory
295 of the platform margin, is not observable in this outcrop, but it is known that this generation of
296 carbonate platforms always presents a downward-concave prograding shoreline trajectory,
297 suggesting a gradual decrease of the accommodation rate (e.g., Bosellini, 1984; Biddle et al., 1992).
298 This observation enables to interpret the L-1 as an highstand systems tract (Fig. 10; Car 2 HST of
299 De Zanche et al. 1993; Gianolla et al. 1998).

300 The upper bed joint of the youngest cliniform of L-1 paleoslope is characterized by the presence of
301 a by-pass surface without evident erosion features (e.g., karst). At Tofana di Rozes, L-2 is
302 dominated by carbonate mounds directly overlaying this surface (Fig. 5) which occur along the
303 whole slope length. Here mounds and arenaceous grainstones of facies L-2 fill the accommodation
304 space up the shelf break of the underlying high-relief platform, from which the cliniforms of facies
305 L-1 originate (Fig. 3). This testifies that, during the deposition of L-2, the sea level was still as high
306 as during the deposition of L-1, so that L-2 is still part of the highstand systems tract of the first
307 depositional sequence (Fig. 10). The difference in the abundance of carbonate mounds vs.
308 arenaceous grainstones observed in L-2 between Tofana di Rozes and Dibona Hut outcrops (Figs. 5;

309 6) is due to their different paleotopographic location. Tofana lies on the high paleo-slope of the
310 Cassian platform, while Dibona was closer to the basin depocenter (Gattolin et al. 2013).

311

312 **5.2 2nd depositional sequence**

313

314 Falling stage systems tract

315

316 The ~ 3 m thick coarse grained interval found at the top of L-2 and representing the onset of mass
317 flow deposits, is interpreted as the beginning of the sea level fall and consequent increase of
318 sediment discharge in the basin. A sharp increase in sediment grain size is testified also at the
319 coeval outcrop of Borca di Cadore and in the whole Cadore area (Neri et al., 2007; Breda et al.,
320 2009b). The basal surface of forced regression (Hunt and Tucker, 1992) can be placed at the base of
321 this coarse grained interval (Fig. 10). At Tofana di Rozes, this surface coincides with a well
322 developed subaerial exposure surface, showing karst (Fig. 8). The clinostratified bedsets, made up
323 of arenaceous grainstones, which constitute the lower portion of the cliff observed at Dibona Hut
324 (L-2-CLINO; Fig. 4), irrespective of their interpretation as a delta body or a coastal prograding
325 wedge, record a fall of the sea level (e.g., Massari et al., 1999; Hernández-Molina et al., 2000;
326 Tropeano and Sabato 2000; Pomar and Tropeano 2001; Massari and D'Alessandro 2010). The
327 offlapping geometry evidences an overall progradation of the shoreline along a descending, low
328 angle trajectory. Consequently, together with the last coarse grained portion of the L-2, the L-2-
329 CLINO represents the falling stage system tract of the second depositional sequence (Fig. 10; Car 3
330 of De Zanche et al. 1993; Gianolla et al. 1998). The stair-stepping surface at the top of the
331 clinostratified sedimentary body (L-2-CLINO; Fig. 4) represents the correlative conformity (*sensu*
332 Hunt and Tucker, 1992, Fig. 10). Being in a paleotopographical higher position with respect to
333 Dibona (Gattolin et al. 2013), the falling stage system tract is not recorded at Tofana di Rozes.
334 Instead, a well developed karst surface is produced by subaerial exposure on top of L-2 (Figs. 8,

335 10). More to the West, e.g., at Falzarego Pass (Fig. 1a), this karstified surface merges with the
336 sequence boundary and lies on top of the platform interior facies of the older Cassian platform, a
337 time equivalent of facies L-1 (Fig. 10).

338

339 Lowstand systems tract

340

341 At Dibona Hut, above the correlative conformity (*sensu* Hunt and Tucker, 1992), the dolomitized
342 arenaceous grainstones beds (L-2-ONLAP; Fig. 4) onlapping the clinofolds represent the base of
343 the lowstand system tract (Fig. 10). This interval, coherently with the paleotopography of the area,
344 deposited only at Dibona Hut which was in a more basinal setting than Tofana di Rozes.

345

346 Transgressive systems tract

347

348 At Dibona Hut, the basal portion of L-3 often displays massive arenites with basal lags, which lie
349 on the karstified top of the underlying peritidal cycles and evolve into the subtidal portion of the
350 following cycle. These are thus interpreted as transgressive lags formed on a formerly emerged
351 coastal area and are evidence of a transgressive ravinement surface (Cattaneo and Steel, 2003). The
352 L-3 marks a sharp change in lithology with respect to the pervasively dolomitized L-2 ONLAP (see
353 Fig. 4c) and is characterized by shallow water peritidal-paralic deposits of tidal-flat/lagoon,
354 cyclically subjected to subaerial exposure and soil development (interval D of Preto and Hinnov,
355 2003; interval 1 of Gattolin et al., 2013). At Tofana di Rozes, L-3 directly overlies in disconformity
356 the karstic surface on top of L-2 and L-1 (i.e. the sequence boundary; Figs. 3; 10). The facies
357 association observed in L-4 is typical of a mainly subtidal environment dominated by tidal currents
358 and therefore identifies a marked deepening of the depositional environment with respect to L-3
359 (interval E-F of Preto and Hinnov 2003; interval 2 of Gattolin et al. 2013). Deepening takes on in L-
360 5, which finer grain-size and nodular bed joints testify the deepest environment of the entire

361 depositional sequence (interval 3 of Gattolin et al. 2013). In this work, L-3 is attributed to the
362 transgressive systems tract because the lag deposits at the base of peritidal cycles are interpreted as
363 minor ravinement surfaces at the beginning of a slow transgression. Thus, Lithozones L-3, L-4 and
364 L-5 represent the transgressive system tract of the second depositional sequence (Fig. 10; Car 3 of
365 De Zanche et al. 1993; Gianolla et al. 1998). Alternatively, these peritidal cycles may be seen as
366 representing tidal-flat and lagoon environments protected by a prograding shoal barrier. In this
367 alternative interpretation, L-3 belongs to the lowstand systems tract and the transgressive systems
368 tract is made up of L-4 and L-5. The maximum flooding surface (Frazier, 1974; Posamentier et al.,
369 1988) is likely placed within L-5 as confirmed by the occurrence of open marine fossils
370 (ammonoids and conodonts; Preto and Hinnov, 2003) and the absence of indicators of high
371 hydraulic energy, implying sedimentation below the wave base.

372

373 Highstand systems tract

374

375 Above, L-6 is coarser grained and characterized by well developed planar to herringbone cross
376 bedding, thus recording a return to shallower conditions with respect to L-5. The observed facies
377 association suggests a subtidal, tide dominated sedimentary environment similar to that of facies
378 association L-4. L-6 is observed in the whole Dolomites area (interval H of Preto and Hinnov, 2003;
379 Neri et al., 2007) and testifies for an important shift of the coast line toward the basins (interval 4 of
380 Gattolin et al. 2013). This lithozone constitutes the HST of the second depositional sequence (Fig.
381 10; Car 3 of De Zanche et al. 1993; Gianolla et al. 1998).

382 The well developed karstic surface on top of L-6 in the study area is observed at a regional scale in
383 the Dolomites and beyond, and is the subaerial unconformity that marks the boundary with the
384 subsequent depositional sequence (Fig. 9; Car 4 of De Zanche et al. 1993; Gianolla et al. 1998).

385 Above it, an abrupt landward shift in facies is observed, with the deposition of the coastal sediments
386 of the Travenanzes Formation, here represented by dm thick beds of aphanitic and mottled

387 dolostones alternated with dark clays (L-7) and suggesting marginal/paralic environments (Breda
388 and Preto, 2011).

389

390 **6. Discussion**

391 6.1 Role of 3D modeling in the study of depositional geometries

392

393 During the last three decades, several interpretations were proposed for the stratigraphic succession
394 outcropping at Dibona Hut, and in particular for the clinostratified body of L-2-CLINO (Fig. 4).

395 Bosellini et al. (1982) and later Doglioni and Carminati (2008) interpreted this body as a

396 tectonically tilted block, bounded by an angular unconformity at its top. Preto and Hinnov (2003)

397 instead interpreted this sedimentary body as a prograding shoal barrier with a tabular geometry. The

398 inaccessibility of this outcrop is the main cause for the lack of an unambiguous interpretation which

399 was carried out on the basis of local observations of sedimentary facies coupled to panoramic views

400 (in the field or on photographs), which are essentially bi-dimensional, and thus affected by

401 perspective distortion. Only the use of three dimensional acquisition and modeling techniques

402 allowed to retrieve quantitative information and observe the true geometry of the outcrop (see in

403 particular L-2-CLINO and L-2-ONLAP in § 4; Fig. 4). The stair stepping surface at the top of L-2-

404 CLINO, which was a key feature to identify and define the falling stage system tract of the second

405 depositional sequence, could only be recognized and traced on the remote-sensed 3D geological

406 model of the outcrop (Fig. 4). Differently from the previous sequence stratigraphic interpretation

407 (De Zanche et al., 1993; Gianolla et al., 1998), the lower portion of the Heiligkreuz Formation is

408 now interpreted to be the last part of the highstand system tract (L-2) of the first depositional

409 sequence (Fig. 10; Car 2 in De Zanche et al., 1993; Gianolla et al., 1998) and not as the lowstand

410 system tract of the second depositional sequence (Car 3 in De Zanche et al., 1993; Gianolla et al.,

411 1998). This is confirmed by the observations carried out from the 3D model of the Tofana di Rozes

412 outcrop. Here, the maximum altitude reached by the mounds of facies L-2, recorded by gps-aided

413 mapping, is the same of the shelf break of the underlying high-relief platform once the original
414 depositional geometry is restored in the 3D environment of the geological model. This implies that
415 during the growth of mounds the sea level was still as high as during the development of the
416 underlying high-relief platform, and so the L-2 s.s. is part of the highstand of the first depositional
417 sequence.

418 Photogrammetry and terrestrial laser scanning are methods which allow the rapid acquisition of
419 field data on a variety of scales, from a metre-scale outcrop to the km scale of a mountain slope.
420 These data can be used as the base for accurate three-dimensional models of sedimentary bodies.
421 Here we have shown that not only 3D acquisition techniques can speed-up the field work and
422 increase accuracy, but also provide the means for interpretations that would be otherwise impossible
423 on inaccessible or exceedingly wide outcrops. In this case, the definition of an accurate sequence
424 stratigraphy across the Carnian Pluvial Event in the Dolomites was only possible using the 3D
425 reconstruction of the outcrops.

426

427 6.2 What triggered the platform demise?

428

429 The demise of the Carnian high-relief carbonate platforms (L-1; the Cassian 2 of De Zanche et al.
430 1993; Gianolla et al. 1998) was attributed by the previous authors (De Zanche et al., 1993; Gianolla
431 et al., 1998) to a subaerial exposure, and a sequence boundary (*sensu* Vail et al., 1991) was placed
432 just above the demised platform and its slopes (base of Car 3 sequence in De Zanche et al., 1993;
433 Gianolla et al., 1998). This work highlighted that the sea level fall occurred at a later stage with
434 respect to the high-relief platform demise. After the Cassian platform demise, small, mainly
435 microbial mounds nucleated all along the abandoned slopes (cf. also Keim et al., 2006). The
436 nucleation of mounds was probably possible because of the shut-down of the underlying high-relief
437 platform (Fig. 5) and interrupted the slope-shedding (Kenter, 1990; Keim et al. 2006). Boulders and
438 other platform-derived sediments, typical of the Cassian platforms (e.g., Reijmer, 1998; Preto,

439 2012), are in fact not found associated with mounds of lithozone L-2. Mounds are rather
440 interfingered with arenaceous grainstones made up of prevailing skeletal grains (Figs. 6; 7), which
441 are only a minor component in the high-relief Cassian platforms (Kenter 1990, Russo et al. 1997,
442 Reijmer 1998; Keim and Schlager 1999, 2001). These observations are confirmed at Lavarella by
443 Keim et al. (2001, 2006; see Fig. 1a for location). Microbial carbonate mounds (Fig. 5) can be
444 interpreted as relics of the Cassian Microbial factory (*sensu* Schlager 2003) that try to hold up the
445 crisis. They are tightly interfingered with arenaceous grainstones that highlight the onset of a
446 important siliciclastic input and of a different carbonate factory producing mostly loose skeletal
447 grains (Figs. 6, 7). At Tofana di Rozes, this unit onlaps the Cassian platform slope up to the shelf
448 break (Fig. 3) and is capped by the same karstic surface found at the top of the Cassian platform
449 (Fig. 8), thus, the main episode of sea level fall is subsequent to the high-relief carbonate platform
450 demise and to the establishment of mounds on the abandoned slope. Sea level fall thus did not
451 trigger the crisis of the high-relief microbial platform.

452

453 In Late Triassic high-relief carbonate platforms of the Dolomites (Cassian *sensu* De Zanche et al.
454 1993), the carbonate production was dominated by microbialites (Russo et al., 1997; Keim and
455 Schlager 1999, 2001). Being independent from light availability, microbialites are less influenced
456 by sea level variations with respect to metazoan reefs. Microbial platforms are usually characterized
457 by a carbonate production zone spread from shallow to deep waters (down to 200-300 m depth;
458 Kenter 1990; Della Porta et al. 2003, 2004; Kenter et al. 2005; Marangon et al. 2011). Data from the
459 geological record demonstrate that carbonate production rates of healthy Tropical and Microbial
460 carbonate factories are high enough to keep the pace of eustatic variations (Schlager 1981; 1999a,b;
461 2003), and in fact the demise of a carbonate platform is generally caused by pulses of tectonic
462 subsidence or by climatic events (Schlager 1981). In the Dolomites, a slow-down of subsidence is
463 observed during the development of the last generations of Carnian high-relief platforms (Bosellini
464 1984; Gianolla and Jacquin, 1998; Bosellini et al. 2003; Stefani et al., 2010). The following

465 depositional sequence (second depositional sequence of this work) testifies the complete filling of
466 sedimentary basins and a flattening of the paleotopography (Fig. 2), so that important subsidence
467 pulses can be excluded. The most probable trigger for the demise of Cassian platforms is thus an
468 episode of climatic change, and specifically the onset of the Carnian Pluvial Event (CPE of Simms
469 and Ruffell 1989; Preto et al. 2010; Dal Corso et al. 2012). The negative carbon isotope excursion
470 that defines the CPE was identified in the Milieres section (Dal Corso et al., 2012), near Rifugio
471 Dibona, and can be traced in the demise surface at the top of the high-relief microbial platform of
472 Tofane. Being a humid period, the CPE determined an increase of hinterland weathering and rivers
473 runoff, reflected in an important input of siliciclastics to the basins. This should have been coupled
474 with an increase in available nutrients which triggered the change of carbonate factory (e.g.,
475 Hallock and Schlager 1986; Mutti and Hallock, 2003; Pomar et al., 2004; Schlager, 2005; Keim et
476 al., 2006).

477

478 At Dibona Hut, mounds were found only under the mass flow deposits and the clinostratified body
479 representing the falling stage systems tract. Above the falling stage systems tract, microbial mounds
480 disappear completely. The demise of the lower Carnian Cassian platforms of the Dolomites was
481 thus a two-step process, in which a first climate and/or oceanographic event (the CPE) killed the
482 km-scale microbial platforms, and then a sea level drop led to the definitive efface of the microbial
483 carbonates. Apart from exposing the shelf, sea level fall may have further stressed the microbial
484 carbonate systems by increasing the siliciclastic and nutrient input.

485

486 6.3 Comparison with Picco di Vallandro and the ecological control on platform geometry

487

488 The change in depositional geometry described in the previous paragraphs is documented also in a
489 few more outcrops of the Dolomites, as the Lavarella slope (Keim et al., 2001; 2006), the eastern
490 flanks of the Sella massif at Passo Campolongo (Keim et al., 2001), and Picco di Vallandro

491 (Rudolph et al., 1989; Biddle et al., 1992). At la Varella and Passo Campolongo unfavourable
492 outcrop conditions prevent a complete reconstruction of this interval, while at Picco di Vallandro,
493 depositional geometries of the early Carnian carbonate platform were carefully reconstructed by
494 Rudolph et al. (1989) and Biddle et al. (1992) (Fig. 11A, B) that recognized repeated episodes of
495 progradation and retrogradation of the platform. They interpreted a sedimentary body of massive
496 dolomite capping the basinal sediments of the San Cassiano Formation as the last episode of strong
497 progradation of the clinostratified high-relief early Carnian platform. An alternative interpretation
498 can be proposed on the basis of the work of Russo et al. (1991) and our own observations. In that
499 view the massive dolomite body lies above a facies association made up of small microbial mounds,
500 skeletal and oolitic grainstones and dark marls (Member A of Russo et al., 1991) which is perfectly
501 comparable to the here described L-2 (§ 4). Since clinofolds are not visible in the field we suggest
502 that the last phase of progradation identified by Rudolph et al. (1989) and Biddle et al. (1992) at
503 Picco di Vallandro is not the last progradation phase of the high-relief platform, but rather
504 represents a low-angle carbonate system bearing small microbial mounds that follows its demise, in
505 analogy to L-2 (§ 4). This unit filled the residual basin initially onlapping the slopes of the high-
506 relief platform at Picco di Vallandro after its demise (Member A of Russo et al., 1991). In the
507 impossibility of identifying internal bedding surfaces, it was interpreted as a strong progradation
508 phase (Rudolph et al., 1989; Biddle et al., 1992). This evolution can be also interpreted in terms of
509 ecological vs. hydrodynamic accommodation (Pomar, 2001; Pomar et al., 2004). The early Carnian
510 high-relief microbial platform built up to sea level, and its steep slopes determined the formation of
511 a well defined basin. During this phase, accommodation can be interpreted as "ecological" on the
512 platform top. After the demise of this platform, however, a mixed sedimentation of shale-sand and
513 loose carbonate grains took place. Being not early cemented, these sediments settled below the
514 wave base, in accordance with a deeper, hydrodynamic equilibrium profile (Pomar, 2001) and thus
515 infilled the residual basins from their bottom. The carbonate body that immediately followed the

516 demise sit on this infilling sequence and extended basinward much more rapidly, and with much
517 less inclined internal bedding, than the underlying platform clinoforms.
518 In sum, sedimentological evidences coupled with changes in the geometry of carbonate bodies
519 recognized in the Cortina area and their comparison to Picco di Vallandro enable to reinterpret the
520 patterns of progradation, basin infilling and ramp development (Fig. 12) at the end of the early
521 Carnian of the Dolomites (Figs. 11; 12) and link them to climatic forcing rather than to changes in
522 sea-level.

523

524 **Acknowledgements**

525

526 Leonardo Tauro and Sebastian Flotow realized thin sections, Andrea Casagrande and Paolo Fedele
527 provided help during fieldwork. Thanks to Matteo Belvedere, Stefano Castelli, Fabio Menna and
528 the 3DOM unit of FBK for sharing their skills on photogrammetry. Giordano Teza for GPS data
529 elaboration. Authors are grateful to Giovanna Della Porta, Guido Roghi, Jacopo Dal Corso,
530 Massimiliano Ghinassi, Manuel Rigo and Silvia Frisia for discussions. Research funded by the
531 MIUR, PRIN project 20107ESMX9_002. Giovanni Gattolin was funded by the CARIPARO
532 foundation.

533

534 **References**

535

536 Biddle, K.T., Schlager, W., Rudolph, K.W., Bush, T.L., 1992. Seismic model of a progradational
537 carbonate platform, Picco di Vallandro, the Dolomites, Northern Italy. AAPG bulletin 76, 14 -30.

538

539 Blendinger, W., 1986. Isolated stationary carbonate platforms: the Middle Triassic (Ladinian) of the
540 Marmolada area, Dolomites, Italy. Sedimentology 33, 159–183.

541

542 Blendinger, W., Brack, P., Norborg, A.K., Wulff-Pedersen, E., 2004. Three-dimensional modelling
543 of an isolated carbonate buildup (Triassic, Dolomites, Italy). *Sedimentology* 51, 297–314.
544

545 Bosellini, A., 1984. Progradation geometries of carbonate platform: example from the Triassic of
546 the Dolomites, Northern Italy. *Sedimentology* 31, 1–24.
547

548 Bosellini, A., dal Cin, R., Gradenigo, A., 1978. Depositi litorali raibliani nella zona di Passo
549 Falzarego (Dolomiti Centrali). *Annali dell'Università di Ferrara* 5, 223-238.
550

551 Bosellini, A., Gianolla, P., Stefani, M., 2003. Geology of the Dolomites. *Episodes* 26, 181-185.
552

553 Bosellini, A., Masetti, D., Neri, C., 1982. La geologia del Passo del Falzarego. In: Castellarin, A.,
554 Vai, G.B. (Eds.), *Guida alla Geologia del Sudalpino Centro-Orientale. Guide geologiche regionali*
555 *della Società Geologica Italiana, Bologna*, pp. 273-278.
556

557 Brack, P., Rieber, H., Mundil, R., Blendinger, W., Maurer, F., 2007. Geometry and chronology of
558 growth and drowning of Middle triassic carbonate platforms (Cernerera and Bivera/Clapsavon) in the
559 southern Alps (northern Italy). *Swiss Journal of Geosciences* 100, 327–347.
560

561 Brandner, R., 1984. Meeresspiegelschwankungen und Tektonik in der Trias der NW-Tethys.
562 *Jahrbuch der Geologischen Bundesanstalt* 126, 435–475.
563

564 Breda, A., Mellere, D., Massari, F., Asioli, A., 2009a. Vertically stacked Gilbert-type deltas of
565 Ventimiglia (NW Italy): the Pliocene record of an overfilled incised valley. *Sedimentary Geology*
566 219, 58-76.
567

568 Breda, A., Preto, N., 2011. Anatomy of an Upper Triassic continental to marginal-marine system:
569 the mixed siliciclastic–carbonate Travenanzes Formation (Dolomites, Northern Italy).
570 *Sedimentology* 58, 1613-1647.
571

572 Breda, A., Preto, N., Roghi, G., Furin, S., Meneguolo, R., Ragazzi, E., Gianolla, P., 2009b. The
573 Carnian Pluvial Event in the Tofane area (Cortina d'Ampezzo, Dolomites, Italy). *Geo. Alp* 6, 80-
574 115.
575

576 Broglio Loriga, C., Cirilli, S., De Zanche, V., Di Bari, D., Gianolla, P., Laghi, G.F., Lowrie, W.,
577 Manfrin, S., Mastandrea, A., Mietto, P., Muttoni, G., Neri, C., Posenato, R., Reichichi, M., Rettori,
578 R., Roghi, G., 1999. The Prati di Stuares/Stuore Wiesen Section (Dolomites, Italy): . global
579 stratotype section and point for the base of the Carnian stage. *Rivista Italiana di Paleontologia e*
580 *Stratigrafia* 105, 37–78.
581

582 Cantalamessa, G., Di Celma, C., Ragaini, L. 2005. Sequence stratigraphy of the Punta Ballena
583 Member of the Jama Formation (Early Pleistocene, Ecuador): insights from integrated
584 sedimentologic, taphonomic and paleoecologic analysis of molluscan shell concentrations.
585 *Palaeogeography, Palaeoclimatology, Palaeoecology* 216, 1-25.
586

587 Cattaneo, A., Steel, R.J., 2003. Transgressive deposits: a review of their variability. *Earth-Science*
588 *Reviews* 62, 187-228.
589

590 Catuneanu, O., 2006. *Principles of Sequence Stratigraphy*. Elsevier, Amsterdam. 375 pp.
591

592 Catuneanu, O., Abreu, V., Bhattacharya, J.P., Blum, M.D., Dalrymple, R.W., Eriksson, P.G.,
593 Fielding, C.R., Fisher, W.L., Galloway, W.E., Gibling, M.R., Giles, K.A., Holbrook, J.M., Jordan,

594 R., Kendall, C.G.St.C, Macurda, B., Martinsen, O.J., Miall, A.D., Neal, J.E., Nummedal, D., Pomar,
595 L., Posamentier, H.W., Pratt, B.R., Sarg, J.F., Shanley, K.W., Steel, R.J., Strasser, A., Tucker, M.E,
596 Winker, C., (2009). Towards the standardization of sequence stratigraphy. *Earth-Science Reviews*,
597 92, 1-33.

598

599 Catuneanu, O., Galloway, W. E., Kendall, C. G., Miall, A. D., Posamentier, H. W., Strasser, A.,
600 Tucker, M. E., 2011. Sequence stratigraphy: methodology and nomenclature. *Newsletters on*
601 *Stratigraphy* 44, 173-245.

602

603 Catuneanu, O., Hancox, P.J., Cairncross, B., Rubidge, B.S., 2002. Foredeep submarine fans and
604 forebulge deltas: orogenic off-loading in the underfilled Karoo Basin. *Journal of African Earth*
605 *Sciences* 35, 489-502.

606

607 Dal Corso, J., Mietto, P., Newton, R.J., Pancost, R.D., Preto, N., Roghi, G., Wignall, P.B., 2012.
608 Discovery of a major negative $\delta^{13}\text{C}$ spike in the Carnian (Late Triassic) linked to the eruption of
609 Wrangellia flood basalts. *Geology* 40, 79-82.

610

611 Della Porta, G., Kenter, J.A.M., Bahamonde, J.R., 2004. Depositional facies and stratal geometry of
612 an Upper Carboniferous prograding and aggrading high-relief carbonate platform (Cantabrian
613 Mountains, N Spain). *Sedimentology* 51, 267–295.

614

615 Della Porta, G., Kenter, J.A.M., Bahamonde, J.R., Immenhauser, A., Villa, E., 2003. Microbial
616 boundstone dominated carbonate slope (Upper Carboniferous, N Spain):microfacies, lithofacies
617 distribution and stratal geometry. *Facies* 49, 175–207.

618

619 Dercourt, J., Ricou, L.E., Vrielynck, B., 1993. Atlas Tethys Palaeoenvironmental Maps.
620 Explanatory Notes. Gauthier-Villars, Paris, 307 pp.
621
622 De Zanche, V., Franzin, A., Gianolla, P., Mietto, P., Siorpaes, C., 1992. The Piz da Peres Section
623 (Valdaora-Olang, Pusteria Valley, Italy): a reappraisal of the Anisian stratigraphy in the Dolomites.
624 *Eclogae Geologicae Helvetiae* 85, 127-143.
625
626 De Zanche, V., Gianolla, P., Manfrin, S., Mietto, P., Roghi, G., 1995. A Middle Triassic
627 backstepping carbonate platform in the Dolomites (Italy): sequence stratigraphy and
628 biochronostratigraphy. *Memorie di Scienze Geologiche* 47, 135– 155.
629
630 De Zanche, V., Gianolla, P., Mietto, P., Siorpaes, C., Vail, P.R., 1993. Triassic sequence
631 stratigraphy in the Dolomites (Italy). *Memorie di Scienze Geologiche* 45, 1-27.
632
633 Doglioni, C., Carminati, E., 2008. Structural style & Dolomites field trip. *Memorie descrittive della*
634 *carta geologica d'Italia volume LXXXII*. APAT, Roma, 295 pp.
635
636 Flügel, E., 2002. Triassic reef patterns. In: Kiessling, W., Flügel, E., Golonka, J. (Eds.),
637 *Phanerozoic Reef Patterns*. SEPM Special Publication 72, pp. 391–463.
638
639 Flügel, E., 2004. *Microfacies of carbonate rocks*. Springer-Verlag, Berlin-Heidelberg (Germany),
640 976 pp.
641
642 Föllmi, K.B., Godet, A., 2013. Paleooceanography of Lower Cretaceous Alpine platform carbonates.
643 *Sedimentology* 60, 131–151.
644

645 Frazier, D.E., 1974. Depositional episodes: their relationship to the Quaternary stratigraphic
646 framework in the northwestern portion of the Gulf Basin. University of Texas at Austin, Bureau of
647 Economic Geology. Geological Circular, vol. 4, 1. 28 pp.
648

649 Gaetani, M., Fois, E., Jadoul, F., Nicora, A., 1981. Nature and evolution of Middle Triassic
650 carbonate buildups in the Dolomites (Italy). *Marine Geology* 44, 25–57.
651

652 Galloway, W.E., 2008. Depositional evolution of the Gulf of Mexico Sedimentary Basin. In: Miall,
653 A.D. (Ed.), *The Sedimentary Basins of the United States and Canada: Sedimentary Basins of the*
654 *World*, v. 5, K. J. Hsu, Series Editor, Elsevier Science Amsterdam, pp. 505–550.
655

656 Galloway, W.E., Williams, T.A., 1991. Sediment accumulation rates in time and space: Paleogene
657 genetic stratigraphic sequences of the northwestern Gulf of Mexico basin. *Geology* 19, 986-989.
658

659 Gattolin, G., Breda, A., Preto, N., 2013. Demise of Late Triassic carbonate platforms triggered the
660 onset of a tide-dominated depositional system in the Dolomites, Northern Italy. *Sedimentary*
661 *Geology* 297, 38-49.
662

663 Gianolla, P., De Zanche, V., Mietto, P., 1998. Triassic sequence stratigraphy in the Southern Alps
664 (northern Italy): definition of sequences and basin evolution. In: De Graciansky, P.C., Hardenbol,
665 J., Jacquin, T., and Vail, P.R. (Eds.), *Mesozoic and Cenozoic Sequence Stratigraphy of European*
666 *Basins*. SEPM Special Publication 60, pp. 719-748.
667

668 Gianolla, P., Jacquin, T., 1998. Triassic sequence stratigraphic framework of western
669 European basins. In: De Graciansky, P.C., Hardenbol, J., Jacquin, T., and Vail, P.R. (Eds.),
670 *Mesozoic and Cenozoic Sequence Stratigraphy of European Basins*. SEPM Special Publication

671 60, pp. 643–650.

672

673 Godet, A., Föllmi, K.B., Spangenberg, J.E., Bodin, S., Vermeulen, J., Adatte, T., Bonvallet, L.,

674 Arnaud, H., 2013. Deciphering the message of Early Cretaceous drowning surfaces from the

675 Helvetic Alps: What can be learnt from platform to basin correlations? *Sedimentology* 60, 152–173.

676

677 Hallock, P., Schlager, W., 1986. Nutrient excess and the demise of coral reefs and carbonate

678 platforms. *Palaios* 1, 389–398.

679

680 Helland-Hansen, W., 1992. Geometry and facies of Tertiary clinothems, Spitsbergen.

681 *Sedimentology* 39, 1013–1029.

682

683 Hernández-Molina, F. J., Fernández-Salas, L. M., Lobo, F., Somoza, L., Díaz-del-Río, V., Dias, J.

684 A., 2000. The infralittoral prograding wedge: a new large-scale progradational sedimentary body in

685 shallow marine environments. *Geo-Marine Letters* 20, 109–117.

686

687 Hornung, T., Krystyn, L., Brandner, R., 2007a. A Tethys-wide mid-Carnian (Upper Triassic)

688 carbonate productivity decline: evidence for the Alpine Reingraben Event from Spiti (Indian

689 Himalaya)? *Journal of Asian Earth Sciences* 30, 285–302.

690

691 Hornung, T., Brandner, R., Krystyn, L., Joachimski, M., Keim, L., 2007b. Multistratigraphic

692 constraints on the NW Tethyan “Carnian crisis”. In: Lucas, S.G., Spielmann, J.A. (Eds.), *The*

693 *Global Triassic: New Mexico Museum of Natural History and Science Bulletin* 41, pp. 59–67.

694

695 Jenkyns, H.C., 1985. The Early Toarcian and Cenomanian-Turonian anoxic events in Europe:

696 comparisons and contrasts. *Geologische Rundschau* 74, 505–518.

697

698 Jenkyns, H.C., 1991. Impact of Cretaceous sea level rise and anoxic events on the Mesozoic
699 carbonate platform of Yugoslavia. *AAPG Bulletin* 75, 1007–1017.

700

701 Keim, L., Brandner, R., Krystyn, L., Mette, W., 2001. Termination of carbonate slope progradation:
702 an example from the Carnian of the Dolomites, Northern Italy. *Sedimentary Geology* 143, 303–323.

703

704 Keim, L., Schlager, W., 1999. Automicrite facies on steep slopes (Triassic, Dolomites, Italy). *Facies*
705 41, 15–25.

706

707 Keim, L., Schlager, W., 2001. Quantitative compositional analysis of a Triassic carbonate platform
708 (Southern Alps, Italy). *Sedimentary Geology* 139, 261–283.

709

710 Keim, L., Spötl, C., Brandner, R., 2006. The aftermath of the Carnian carbonate platform demise: a
711 basinal perspective (Dolomites, Southern Alps). *Sedimentology* 53, 361–386.

712

713 Kenter, J.A.M., 1990. Carbonate platform flanks: slope angle and sediment fabric. *Sedimentology*
714 37, 777–794.

715

716 Kenter, J.A.M., Harris, P.M., Della Porta, G., 2005. Steep microbial boundstonedominated platform
717 margins - examples and implications. *Sedimentary Geology* 178, 5-30.

718

719 Léonide, P., Floquet, M., Durlet, C., Baudin, F., Pittet, B., Lécuyer, C., 2012. Drowning of a
720 carbonate platform as a precursor stage of the Early Toarcian global anoxic event (Southern
721 Provence sub-Basin, South-east France). *Sedimentology* 59, 156–184.

722

723 Marangon, A., Gattolin, G., Della Porta, G., Preto, N., 2011. The Latemar: A flat-topped, steep
724 fronted platform dominated by microbialites and synsedimentary cements. *Sedimentary Geology*
725 240, 97–114.
726

727 Masetti, D., Neri, C., 1980. L'Anisico della Val di Fassa (Dolomiti occidentali): sedimentologia e
728 paleogeografia. *Annali Università Ferrara* 9, 1–19.
729

730 Massari, F., D'Alessandro, A., 2010. Icehouse, cool-water carbonate ramps: the case of the Upper
731 Pliocene Capodarso Fm (Sicily): role of trace fossils in the reconstruction of growth stages of
732 prograding wedges. *Facies* 56, 47-58.
733

734 Massari, F., Sgavetti, M., Rio, D., D'alessandro, A., Prosser, G., 1999. Composite sedimentary
735 record of falling stages of Pleistocene glacio-eustatic cycles in a shelf setting (Croton basin, south
736 Italy). *Sedimentary Geology* 127, 85-110.
737

738 Mateu-Vicens, G., Pomar, L., Tropeano, M., 2008. Architectural complexity of a carbonate
739 transgressive systems tract induced by basement physiography. *Sedimentology* 55, 1815-1848.
740

741 Mellere, D., Steel, R., 1995. Variability of lowstand wedges and their distinction from forced-
742 regressive wedges in the Mesaverde Group, southeast Wyoming. *Geology* 23, 803-806.
743

744 Miall, A. D., Arush, M., 2001. The Castlegate Sandstone of the Book Cliffs, Utah: sequence
745 stratigraphy, paleogeography, and tectonic controls. *Journal of Sedimentary Research* 71, 537-548.
746

747 Miall, A. D., Catuneanu, O., Vakarelov, B., Post, R., 2008. The Western Interior Basin. In: Miall,
748 A.D. (Eds.), *The Sedimentary Basins of the United States and Canada: Sedimentary basins of the*
749 *World*, v. 5, K. J. Hsü, Series Editor, Elsevier Science, Amsterdam, pp. 329–362.

750

751 Mutti, M., Bernouilli, D., Stille, P., 1997. Temperate carbonate platform drowning linked to
752 Miocene oceanographic events: Maiella platform margin, Italy. *Terra Nova* 9, 122–125.

753

754 Mutti, M., Droxler, A.W., Cunningham, A.D., 2005. Evolution of the Northern Nicaragua Rise
755 during the Oligocene-Miocene: drowning by environmental factors. *Sedimentary Geology* 175,
756 237–258.

757

758 Mutti, M., Hallock, P., 2003. Carbonate systems along nutrients and temperature gradients: some
759 sedimentological and geochemical constraints. *International Journal of Earth Sciences (Geologische*
760 *Rundschau)* 92, 465–475.

761

762 Muttoni, G., Kent, D.V., Channell, J.E., 1996. Evolution of Pangea: paleomagnetic constraints from
763 the Southern Alps, Italy. *Earth and Planetary Science Letters* 140, 97-112.

764

765 Nakada, R., Ogawa, K., Suzuki, N., Takahashi, S., Takahashi, Y., 2014. Late Triassic compositional
766 changes of aeolian dusts in the pelagic Panthalassa: Response to the continental climatic change,
767 *Palaeogeography, Palaeoclimatology, Palaeoecology* 393, 61-75.

768

769 Neri, C., Gianolla, P., Furlanis, S., Caputo, R., Bosellini, A., 2007. Note illustrative della Carta
770 Geologica d'Italia alla scala 1:50000, foglio 029 Cortina d'Ampezzo. APAT, Roma, 200 pp.

771

772 Neri, C., Stefani, M., 1998. Sintesi cronostratigrafica e sequenziale dell'evoluzione permiana
773 superiore e triassica delle Dolomiti. *Memorie Società Geologica Italiana* 53, 417–463.
774

775 Pasquier, J.B., Strasser, A., 1997. Platform-to-basin correlation by high-resolution sequence
776 stratigraphy and cyclostratigraphy (Berriasian, Switzerland and France). *Sedimentology* 44, 1071-
777 1092.
778

779 Pomar, L., 2001. Ecological control of sedimentary accommodation: evolution from a carbonate
780 ramp to rimmed shelf, Upper Miocene, Balearic Islands. *Palaeogeography, Palaeoclimatology,*
781 *Palaeoecology* 175, 249-272.
782

783 Pomar, L., Brandano, M., Westphal, H., 2004. Environmental factors influencing skeletal-grain
784 sediment associations: a critical review of Miocene examples from the Western-Mediterranean.
785 *Sedimentology* 51, 627–651
786

787 Pomar, L., Tropeano, M., 2001. The Calcarene di Gravina Formation in Matera (southern Italy):
788 new insights for coarse-grained, large-scale, cross-bedded bodies encased in offshore deposits.
789 *AAPG bulletin* 85, 661-689.
790

791 Posamentier, H.W., Jervey, M.T., Vail, P.R., 1988. Eustatic controls on clastic deposition
792 I—conceptual framework. In: Wilgus, C.K., Hastings, B.S., Kendall, C.G.St.C., Posamentier,
793 H.W., Ross, C.A., Van Wagoner, J.C. (Eds.), *Sea Level Changes—An Integrated Approach*. Special
794 Publication, vol. 42. Society of Economic Paleontologists and Mineralogists (SEPM), pp. 110–124.
795

796 Preto, N., 2012. Petrology of carbonate beds from the stratotype of the Carnian (Stuores Wisen
797 section, Dolomites, Italy): the contribution of platform-derived microbialites. *Geo. Alp* 9, 12-29.

798

799 Preto, N., Franceschi, M., Gattolin, G., Massironi, M., Riva, A., Gramigna, P., Bertoldi, L., Nardon,
800 S., 2011. The Latemar: a Middle Triassic polygonal fault-block platform controlled by
801 synsedimentary tectonics. *Sedimentary Geology* 234, 1–18.

802

803 Preto, N., Hinnov, L.A., 2003. Unraveling the origin of carbonate platform cyclothems in the Upper
804 Triassic Durrenstein Formation (Dolomites, Italy). *Journal of Sedimentary Research* 73, 774-789.

805

806 Preto, N., Kustatscher, E., Wignall, P.B., 2010. Triassic climates - State of the art and perspectives.
807 *Palaeogeography, Palaeoclimatology, Palaeoecology* 290, 1-10.

808

809 Preto, N., Spötl, C., Mietto, P., Gianolla, P., Riva, A., Manfrin, S., 2005. Aragonite dissolution,
810 sedimentation rates and carbon isotopes in deep-water hemipelagites (Livinallongo Formation,
811 Middle Triassic, northern Italy). *Sedimentary Geology* 181, 173-194.

812

813 Prochnow, S.J., Nordt, L.C., Atchley, S.C., Hudec, M.R., 2006. Multi-proxy paleosol evidence for
814 Middle and Late Triassic climate trends in eastern Utah. *Palaeogeography, Palaeoclimatology,*
815 *Palaeoecology* 232, 53–72.

816

817 Reijmer, J.J.G., 1998. Compositional variations during phases of progradation and retrogradation of
818 a Triassic carbonate platform (Picco di Vallandro/Durrenstein, dolomites, Italy). *Geologische*
819 *Rundschau* 87, 436–448.

820

821 Rigo, M., Joachimski, M.M., 2010. Palaeoecology of Late Triassic conodonts: Constraints from
822 oxygen isotopes in biogenic apatite. *Acta Palaeontologica Polonica* 55, 471-478.

823

824 Roghi, G., 2004. Palynological investigations in the Carnian of the Cave del Predil area (Julian
825 Alps, NE Italy). *Review of Palaeobotany and Palynology* 132, 1–35.

826

827 Rudolph, K.W., Schlager, W., Biddle, K.T., 1989. Seismic models of a carbonate foreslope-to-basin
828 transition, Picco di Vallandro, Dolomite Alps, northern Italy. *Geology* 17, 453-456.

829

830 Ruffer, T., Zühlke, R., 1995. Sequence stratigraphy and sea-level changes in the Early to Middle
831 Triassic of the Alps: a global comparison. In: Haq, B.U. (Ed.), *Sequence Stratigraphy and*
832 *Depositional Response to Eustatic, Tectonic and Climatic Forcing*. Kluwer, Amsterdam, pp. 161–
833 207.

834

835 Russo, F., Neri, C., Mastandrea, A., Baracca, A., 1997. The mudmound nature of the Cassian
836 platform margins of the Dolomites. A case history: the Cipit boulders from Punta Grohmann (Sasso
837 Piatto Massif, Northern Italy). *Facies* 36, 25–36.

838

839 Russo, F., Neri, C., Mastandrea, A., Laghi, G., 1991. Depositional and diagenetic history of the
840 Alpe di Specie (Seelandalpe) fauna (Carnian, northeastern Dolomites). *Facies* 25, 187-210.

841

842 Schlager, W., 1981. The paradox of drowned reefs and carbonate platforms. *Geological Society of*
843 *America Bulletin* 92, 197-211.

844

845 Schlager, W., 1991. Depositional bias and environmental change - important factors in sequence
846 stratigraphy. *Sedimentary Geology* 70, 109-130.

847

848 Schlager, W., 1993. Accommodation and supply - a dual control on stratigraphic sequences.
849 *Sedimentary Geology* 86, 111-136.

850

851 Schlager, W., 1999a. Scaling of sedimentation rates and drowning of reefs and carbonate platforms.
852 *Geology* 27, 183–6.

853

854 Schlager, W., 1999b. Type 3 sequence boundarbies. In: Harris, P.M., Sallet, A.H., Simo, T. (Eds.),
855 *Advances in Carbonate Sequence Stratigraphy: Application to Reservoirs, Outcrops and Models*.
856 *SEPM Special Publication* 63, 35–45.

857

858 Schlager, W., 2003. Benthic carbonate factories of the Phanerozoic. *International Journal of Earth*
859 *Sciences* 92, 445-464.

860

861 Schlager, W., 2005. Carbonate sedimentology and sequence stratigraphy. *SEPM concept in*
862 *sedimentology and paleontology* 8, 200 pp.

863

864 Schlager, W., Reijmer, J.J.G., Droxler, A., 1994. Highstand shedding of carbonate platforms.
865 *Journal of Sedimentary Research* 64, 270-281.

866

867 Schlager, W., Schöllnberger, W., 1974. Das Prinzip stratigraphischer Wenden in der Schichtfolge
868 der Nördlichen Kalkalpen. *Mitteilungen. Österreichische Geologische Gesellschaft* 66–67, 165–
869 193.

870

871 Simms, M.J., Ruffell, A.H., 1989. Synchronicity of climatic change and extinctions in the Late
872 Triassic. *Geology* 17, 265-268.

873

874 Simms, M.J., Ruffell, A.H., 1990. Climatic and biotic change in the late Triassic. *Journal of the*
875 *Geological Society of London* 147, 321–327.

876

877 Simms, M.J., Ruffel, A.H., Johnson, L.A., 1995. Biotic and climatic changes in the Carnian
878 (Triassic) of Europe and adjacent areas. In: Fraser, N.C., Sues, H.D. (Eds.), *In the Shadow of the*
879 *Dinosaurs: Early Mesozoic Tetrapods*. Cambridge University Press, pp. 352–365.

880

881 Stefani, M., Furin, S., Gianolla, P., 2010. The changing climate framework and depositional
882 dynamics of Triassic carbonate platforms from the Dolomites. *Palaeogeography,*
883 *Palaeoclimatology, Palaeoecology* 290, 43-57.

884

885 Tropeano, M., Sabato, L., 2000. Response of Plio-Pleistocene mixed bioclastic-lithoclastic
886 temperate-water carbonate systems to forced regressions: the Calcarene di Gravina Formation,
887 Puglia, SE Italy. In: Hunt, D., Gawthorpe, R.L. (Eds.), *Sedimentary responses to forced regressions,*
888 *Geological Society, London, Special Publications* 172, 217-243.

889

890 Tucker, M.E., Wright, V.P., 1990. *Carbonate sedimentology*. Blackwell, Oxford, 492 pp.

891

892 Vail P.R., Audemard, F., Bowman, S.A, Eisner, P.N., Perez Cruz, C., 1991. The stratigraphic
893 signatures of tectonics, eustasy and sedimentology-an overview. In: G. Einsele, G., Ricken, W.,
894 Seilacher, A. (Eds.), *Cycles and events in stratigraphy*, Springer-Verlag, Berlin-Heidelberg, pp.
895 617-659.

896

897 Weissert, H., Lini, A., Föllmi, K.B., Kuhn, O., 1998. Correlation of Early Cretaceous carbon
898 isotope stratigraphy and platform drowning events: a possible link? *Palaeogeography,*
899 *Palaeoclimatology, Palaeoecology* 137, 189–203.

900

901 Wilson, P.A., Jenkyns, H.C., Elderfield, H., Larson, R.L., 1998. The paradox of drowned carbonate
902 platforms and the origin of Cretaceous Pacific guyots. *Nature* 392, 889–94.

903

904 Ziegler, P.A., 1988. Evolution of the Arctic-North Atlantic and Western Tethys. *AAPG Memoir* 43,
905 Tulsa, pp. 164- 196.

906

907 **Captions**

908

909 Fig. 1. (A) Location and map of the study area. Stars indicate the studied outcrops (see Fig. 3A,
910 4A), triangles the major mountain tops (elevations in meters) and dots the main towns. (B) Position
911 of the Dolomites during Middle-Late Triassic.

912

913 Fig. 2. Lithostratigraphic scheme (modified from Preto and Hinnov, 2003) of the studied interval in
914 the Cortina-Tofane area. The Heiligkreuz Formation, is highlighted in grey. The platform (to the
915 left) corresponds to Tofana di Rozes area, the basin (to the right) corresponds to Dibona Hut area.
916 Ammonoid symbols indicate ammonoid occurrences in the area. (A) Names of lithostratigraphic
917 units (from Neri et al., 2007). (B) Ammonoid biostratigraphy (from Mietto and Manfrin, 1995). (C-
918 D) Chronostratigraphy stages and substages. The clinostatified body of Dibona Hut was
919 represented with tabular progradation in Preto and Hinnov (2003) but is here reinterpreted as a
920 clinostatified prograding body with descending trajectory of the shelf edge (see L-2 clino in § 4
921 and Fig. 4C, and § 5).

922

923 Fig. 3. (A) The outcrop on the southern wall of the Tofana di Rozes. The white rectangle indicates
924 the area of interest i.e. the stratigraphic interval object of this study. (B) Photogrammetric three
925 dimensional model of the outcrop (only the area of interest was modeled). (C) Line drawing of the

926 outcrop. Black dashed lines indicate the lithozones limits (see the § 4 for a description of facies and
927 stratal relationships). F7 indicates the location of Fig. 7.

928

929 Fig. 4. (A) The Dibona Hut outcrop. (B) Three dimensional model of the outcrop. This model is a
930 three dimensional point cloud obtained by a terrestrial laser scanner. (C) Line drawing of the
931 outcrop. Black dashed lines indicate the lithozones limits, grey continuous lines the bedding in the
932 second lithozone (see § 4 for a description of facies and stratal relationships).

933

934 Fig. 5. Outcrops at the boundary between L-1 and L-2 at Tofana di Rozes and their interpretation.
935 The boundary between L-1 and L-2 is constituted by a E dipping by-pass surface which developed
936 on the top of the youngest L-1 clinoform. This surface is onset by lenticular-shaped carbonate
937 bodies (mounds) mainly made up of microbial boundstone.

938

939 Fig. 6. (A) Outcrop of L-2 at Dibona Hut and (B) its interpretation. Lenticular-shaped carbonate
940 bodies (mounds) mainly made up of microbial boundstone are interlayered and laterally overlapped
941 by dm thick beds of arenaceous grainstones.

942

943 Fig. 7. (A) Stratigraphic log of a loose sediment intercalation in the L-2 at Tofana di Rozes and (B)
944 a detail of it. This intercalation lies between two carbonate mounds and is mainly made up of cm-
945 dm thick beds of grainstone (and its dolomitized counterpart), arenaceous grainstones, calcisiltite
946 and shales. The location of this stratigraphic log is highlighted in Fig. 3C.

947

948 Fig. 8. (A) Western portion of Tofana di Rozes outcrop and (B) its interpretation. Here the L-1 is
949 directly overlaid by the L-3. The boundary between L-1 and L-3 is constituted by a karstic surface.

950

951 Fig. 9. Karst at the top of the L-6 at Lastoni di Formin (see Fig. 1A for location).

952

953 Fig. 10. Sequence stratigraphic correlation of three schematic stratigraphic logs representing the
954 sequences outcropping at Tofana di Rozes, Dibona Hut and Lastoni di Formin/Falzarego
955 Pass/Valparola Pass (see Fig. 1a for locations). The Lastoni di Formin/Falzarego Pass/Valparola
956 Pass log has been summarized according to Bosellini et al (1978), Preto and Hinnov (2003);
957 Gattolin et al. (2013). The figure not in scale, the thickness of lithozones is only indicative. HST =
958 highstand system tract, FSST = falling stage system tract, LST= lowstand system tract, TST =
959 trasgressive system tract. SU = subaerial unconformity, BSFR = basal surface of forced regression
960 (Hunt and Tucker, 1992), CC = correlative conformity (*sensu* Hunt and Tucker 1992), TRS =
961 trasgressive ravinement surface (Cattaneo and Steel, 2003); MFS = maximum flooding surface
962 (Frazier, 1974; Posamentier et al., 1988). In this scheme the L-2 has been comprised in the TST but
963 it can be alternatively considered as part of the LST (see § 5).

964

965 Fig. 11. (A) Interpretation of the Picco di Vallandro area modified from Rudolph et al. (1989) and
966 Biddle et al., (1992). The Cassian 2 (*sensu* De Zanche et al., 1993) is the last generation of Carnian
967 high-relief carbonate platforms (L-1 in this paper), its basinal equivalent is the San Cassiano Fm.
968 (De Zanche et al., 1993); Heiligkreuz Fm. is used *sensu* Neri et al. (2007) and corresponds to the
969 lithozones from L-2 to L-6 described in this paper (see Fig. 2 for details on stratigraphy). (B) Detail
970 of the South-western sector modified from the Fig. 5 of Biddle et al. 1992 displaying the closure of
971 the basin and the consequent end of the high-relief platform progradation. (C) New interpretation of
972 the Picco di Vallandro area according to Russo et al., (1991) and our own data. Member A of Russo
973 et al., (1991) corresponds to the interval between the surface of demise of high-relief platforms and
974 the base of the falling stage systems tract, in turn correspondent to the L-2 of this paper. Thus the
975 infilling of the basin is subsequent to the high-relief platform demise and the change in depositional
976 geometry is related to the climate change triggering the carbonate factory turnover.

977

978 Fig. 12. Schematic reconstruction of the key depositional phases observed in the studied
979 stratigraphic interval.

Figure 1

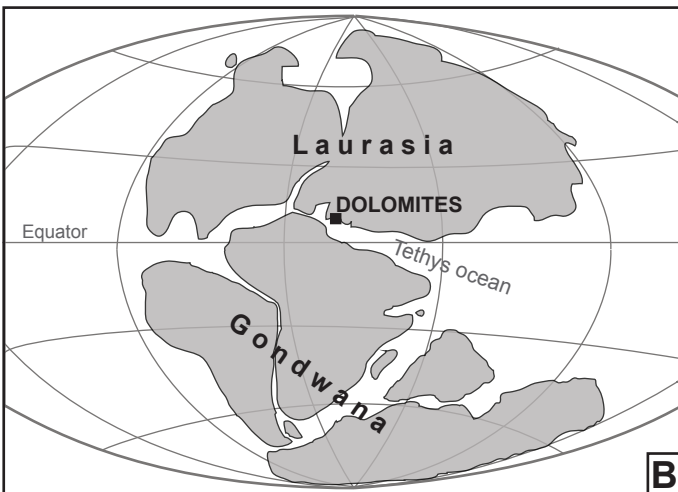
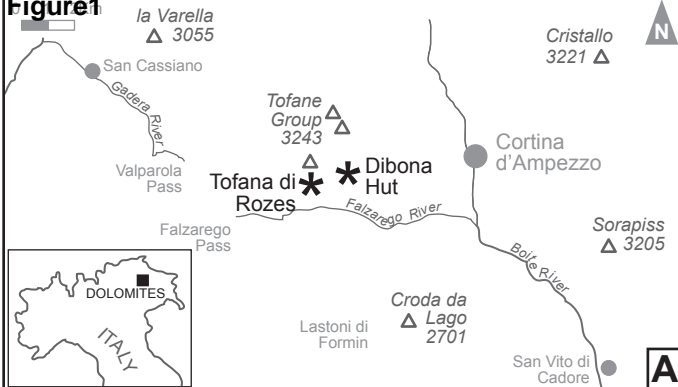
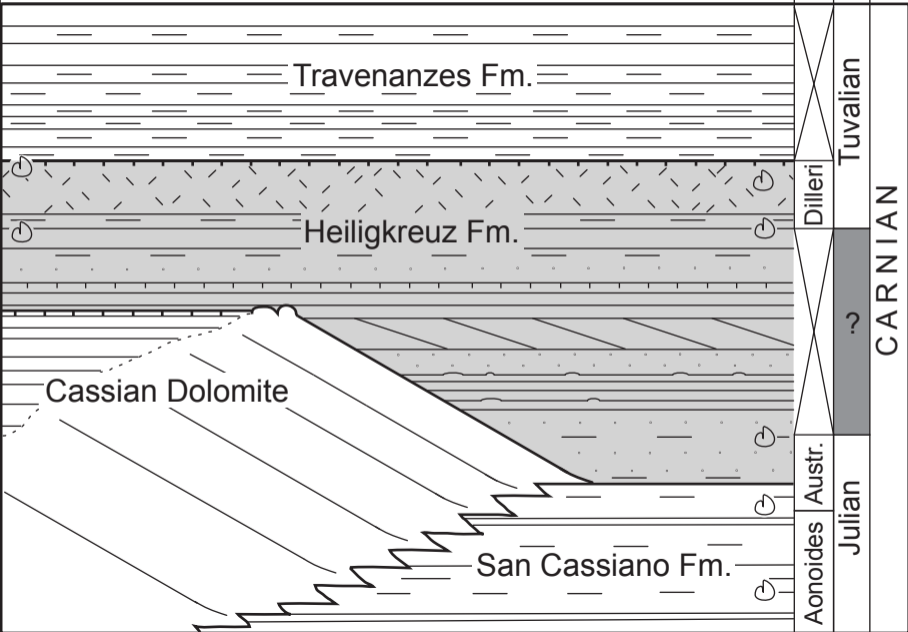


Figure2

A

B C D



Travenanzes Fm.

Heiligkreuz Fm.

Cassian Dolomite

San Cassiano Fm.

Dilleri

Aonoides Austr.

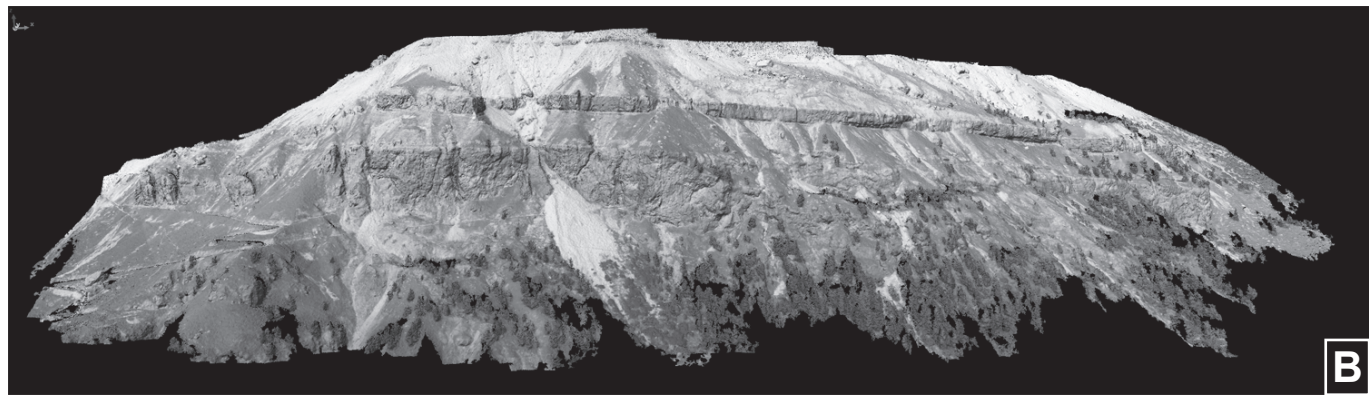
Tuvaian

Julian

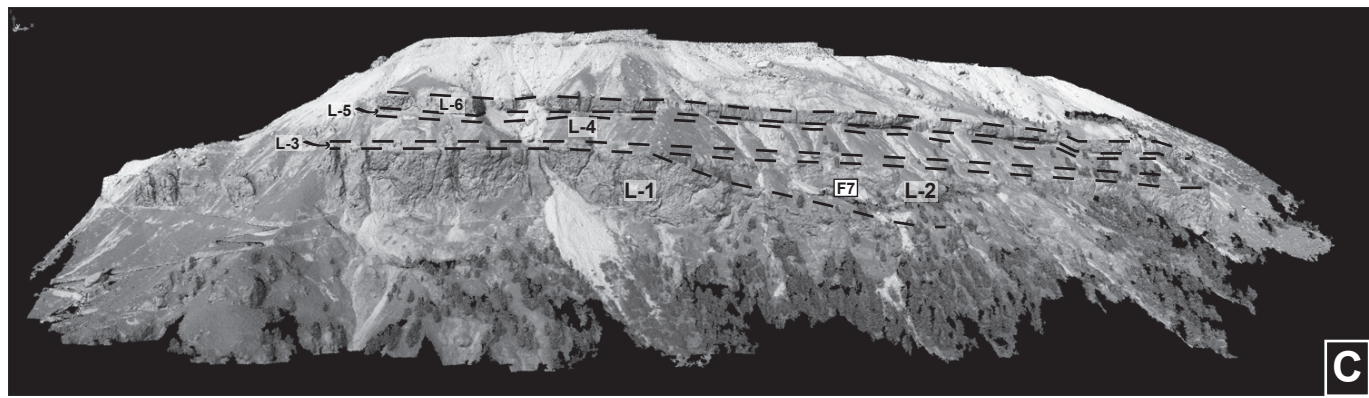
CARNIAN



A



B



C

Figure 4

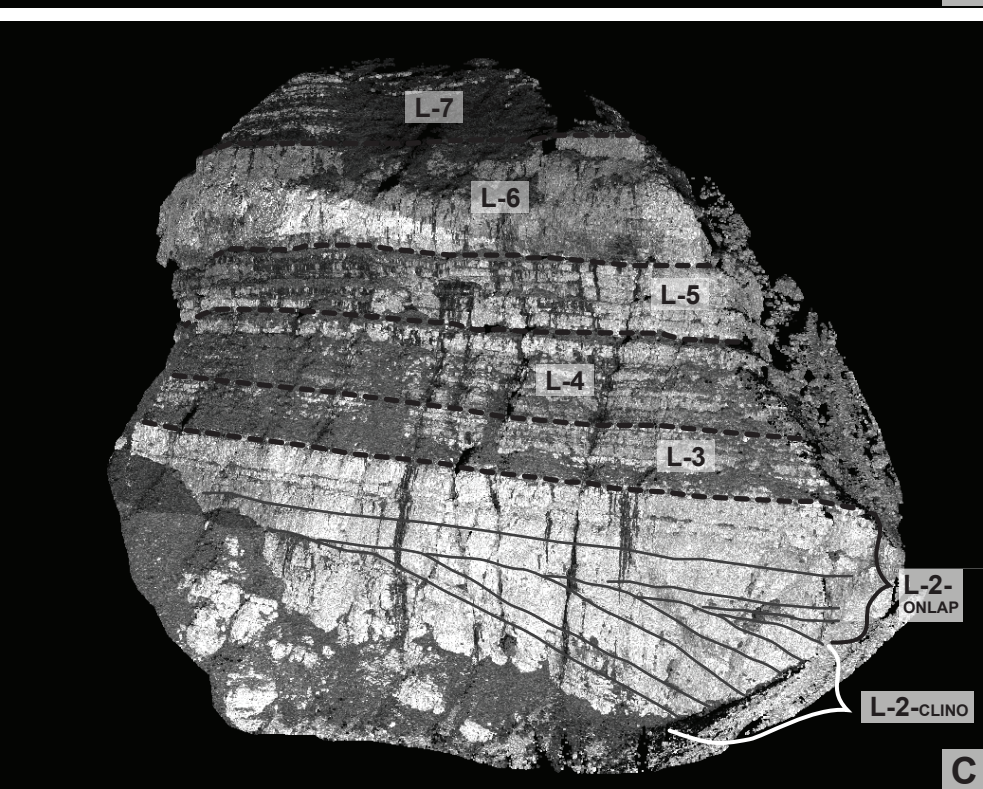
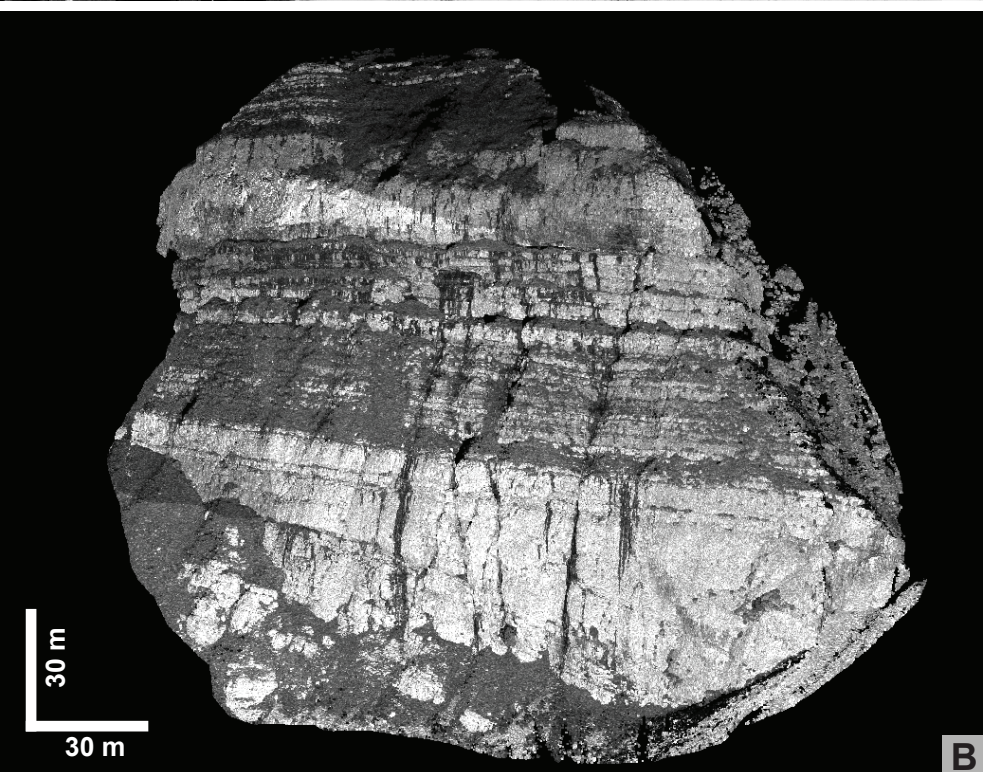
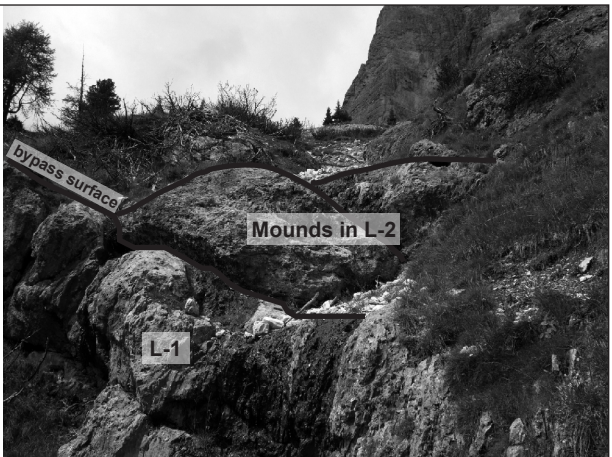


Figure5



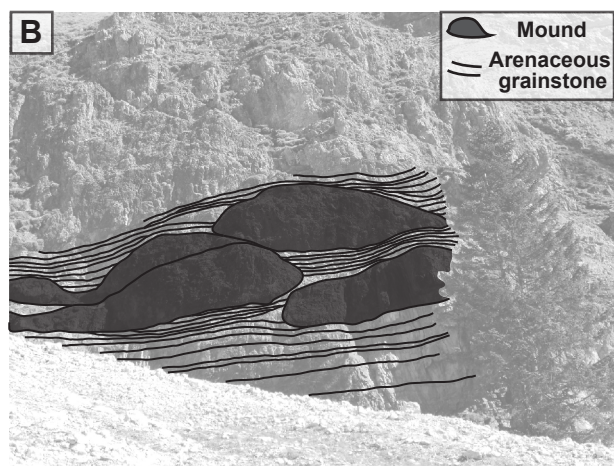


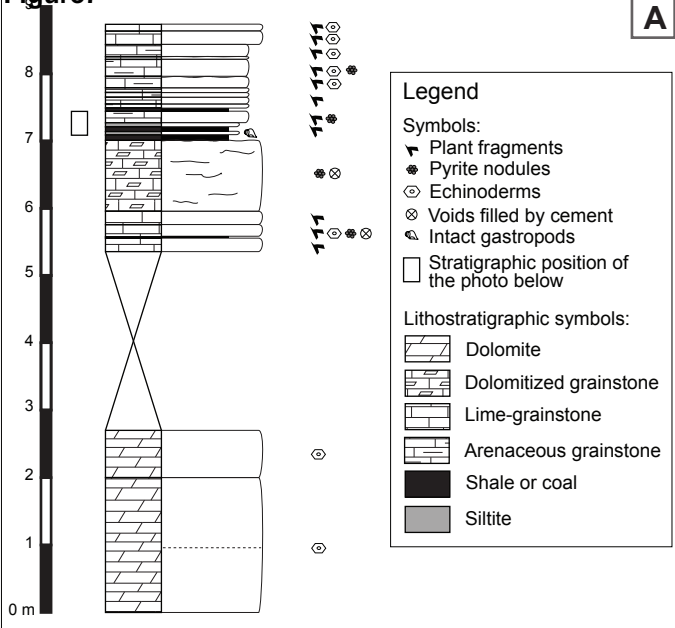
Figure 7**A****B**

Figure 8

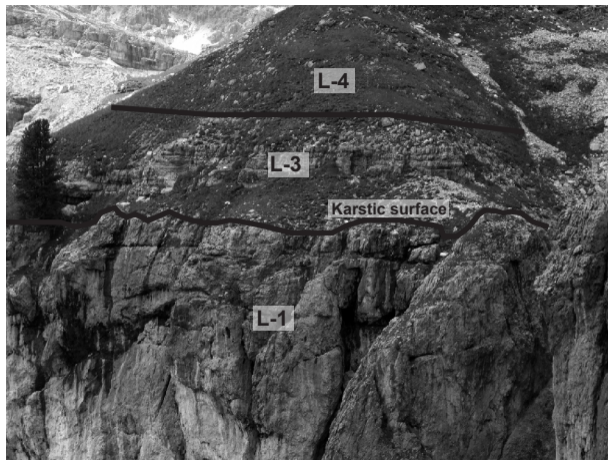
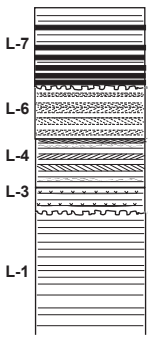


Figure9

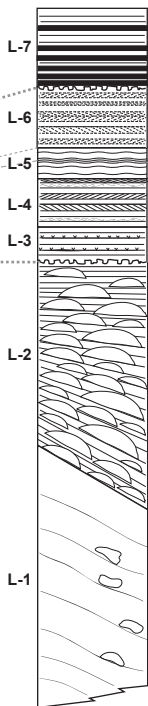


Figure 10
 di Formini

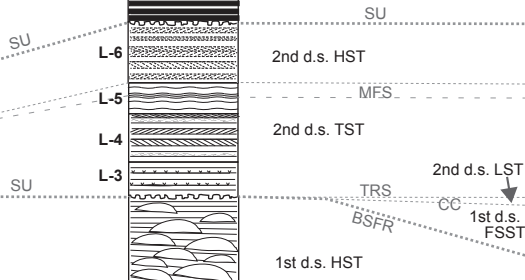
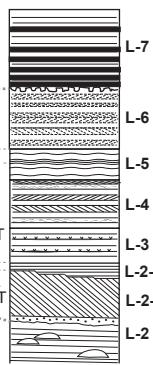
Falzarego and
 Valparola Pass



Tofana di
 Rozes



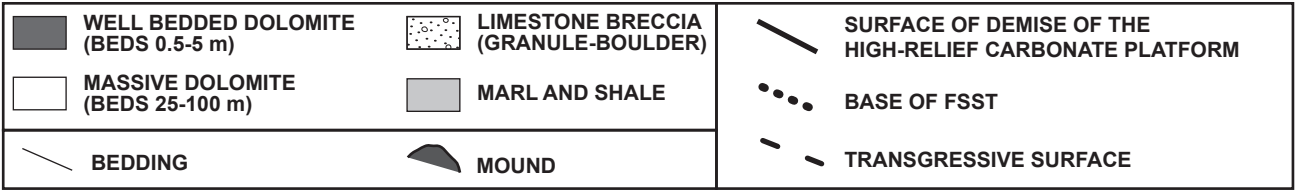
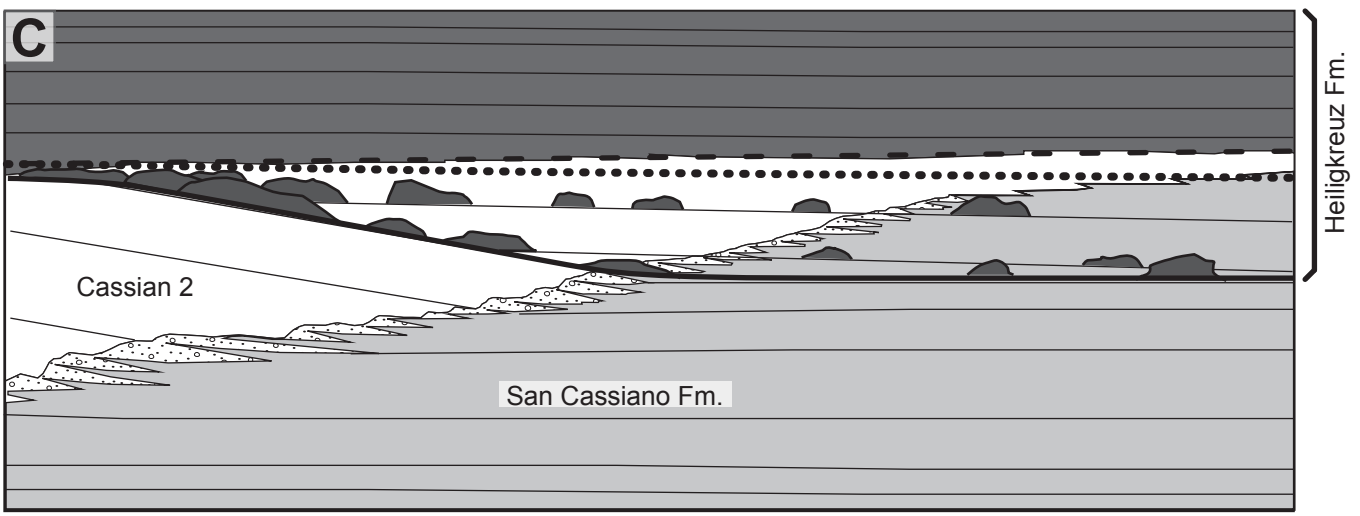
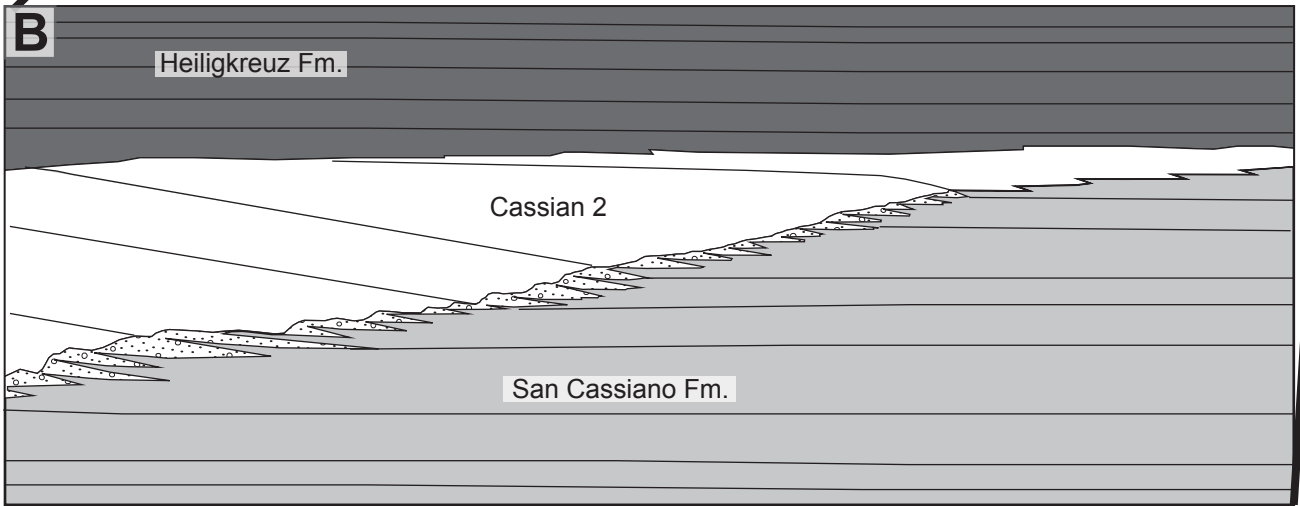
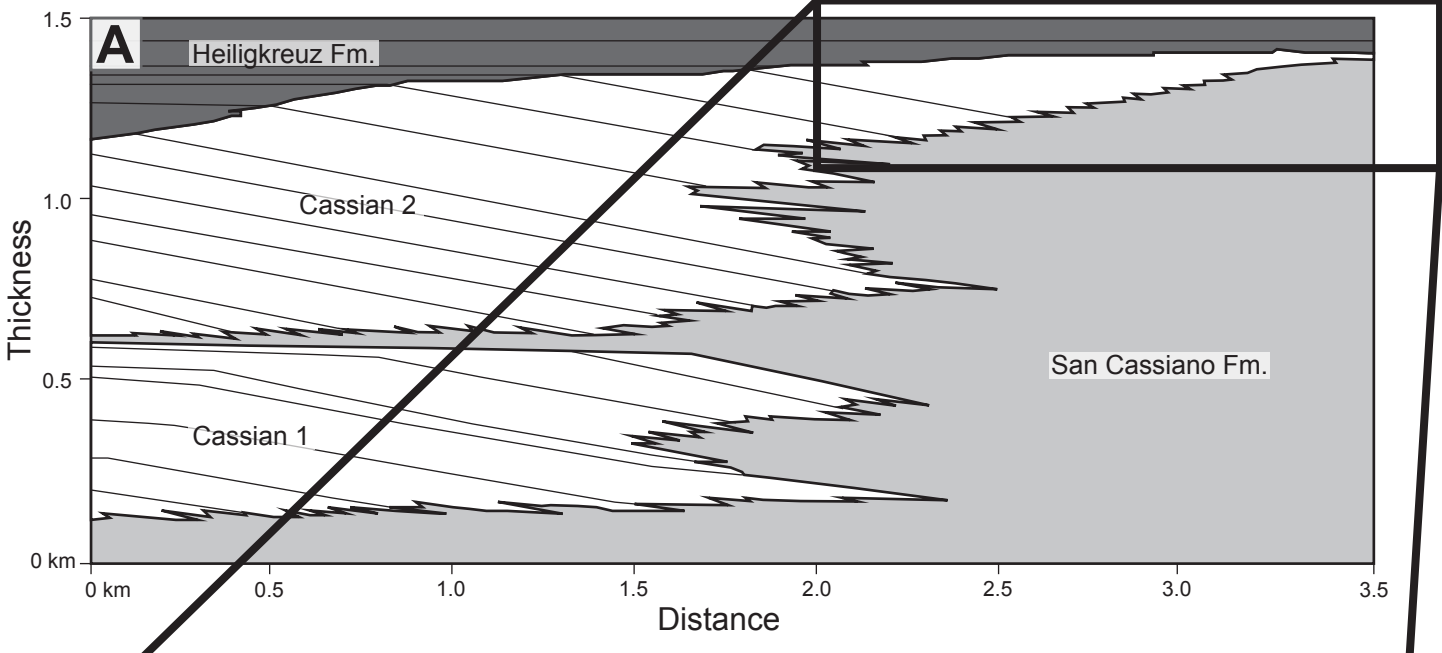
Dibona Hut

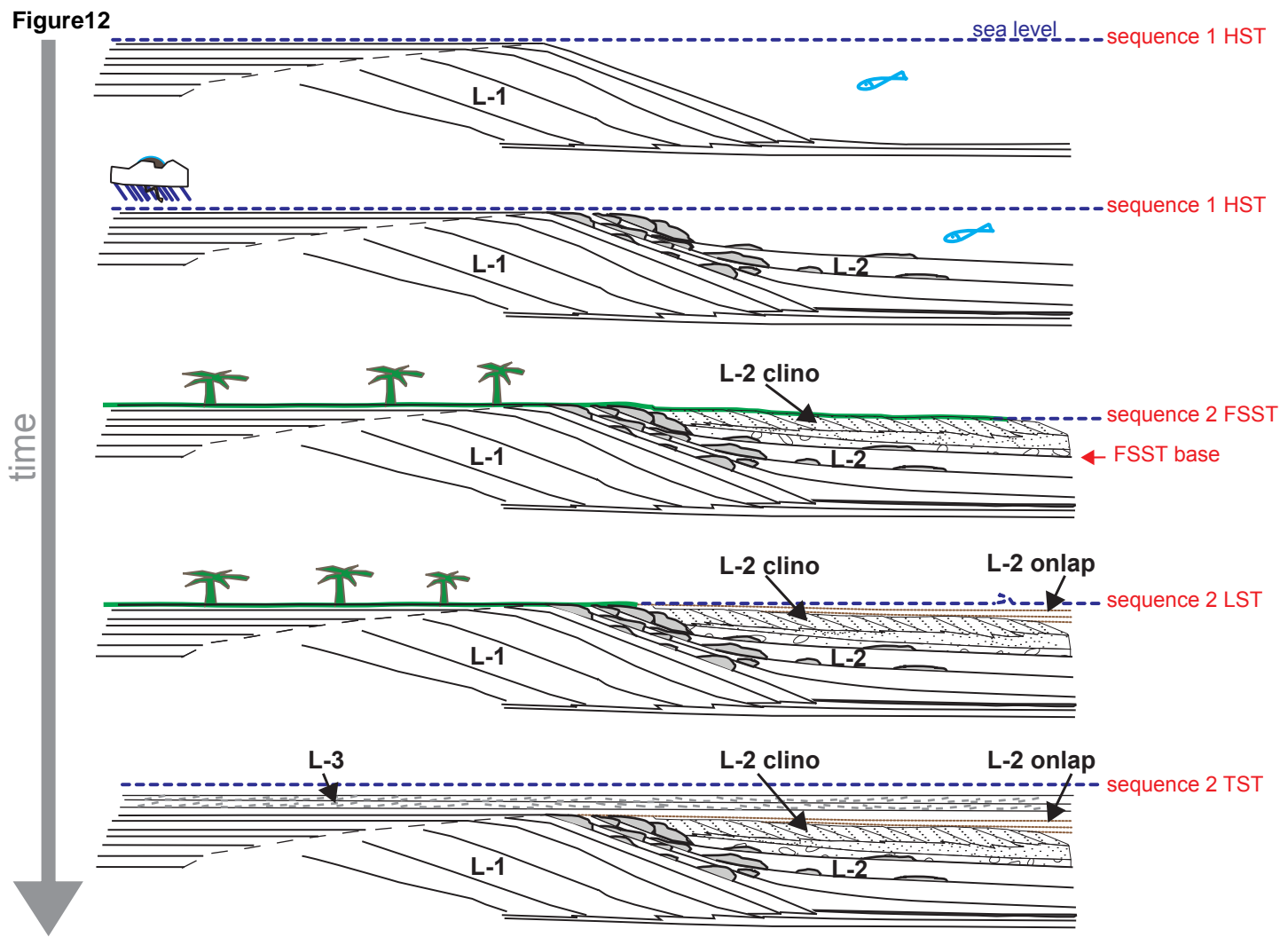


Legend

- Erosive surface
- Karstic surface
- Clay-shale-siltite
- Mound
- Olistolith
- Plane parallel bed joints
- Undulate bed joints
- Inclined bed joints
- Soil
- Cross bedding
- Flaser-wavy bedding
- System tract limit
- Lithozone limit
- L-3** Lithozone name

Figure 1.1 NE SW





Legend

- | | | | |
|--|---|---|---|
|  Mound |  Clinostratified grainstones |  Coarse grained facies |  Cross stratification |
|  Platform margin |  Subaerial exposure | L-1 Lithozone name |  Climate change (rainfall increase) |